Advances in FDTD Techniques and Applications in Photonics

Allen Taflove

Department of Electrical Engineering and Computer Science

Northwestern University, Evanston, IL 60208

Presented at:

Photonics North 2007
Ottawa, Canada

June 4, 2007

Paper Number 1: Kane Yee
IEEE Trans. Antennas & Propagation, May 1966

Numerical Solution of Initial Boundary Value Problems Involving Maxwell's Equations In Isotropic Media

KANE S. YEE

Abstract—Maxwell's equations are replaced by a set of finite difference equations. It is shown that if one chooses the field points appropriately, the set of finite difference equations is applicable for a boundary condition involving perfectly conducting surfaces. An example is given of the scattering of an electromagnetic pulse by a perfectly conducting cylinder.

obstacle is moderately large compared to that of an incoming wave.

A set of finite difference equations for the system of partial differential equations will be introduced in the early part of this paper. We shall then show that with an

2839 citations as of April 26, 2007: ~350 citations in the previous 12 months
(Source: ISI Web of Science)

Yearly FDTD-Related Publications

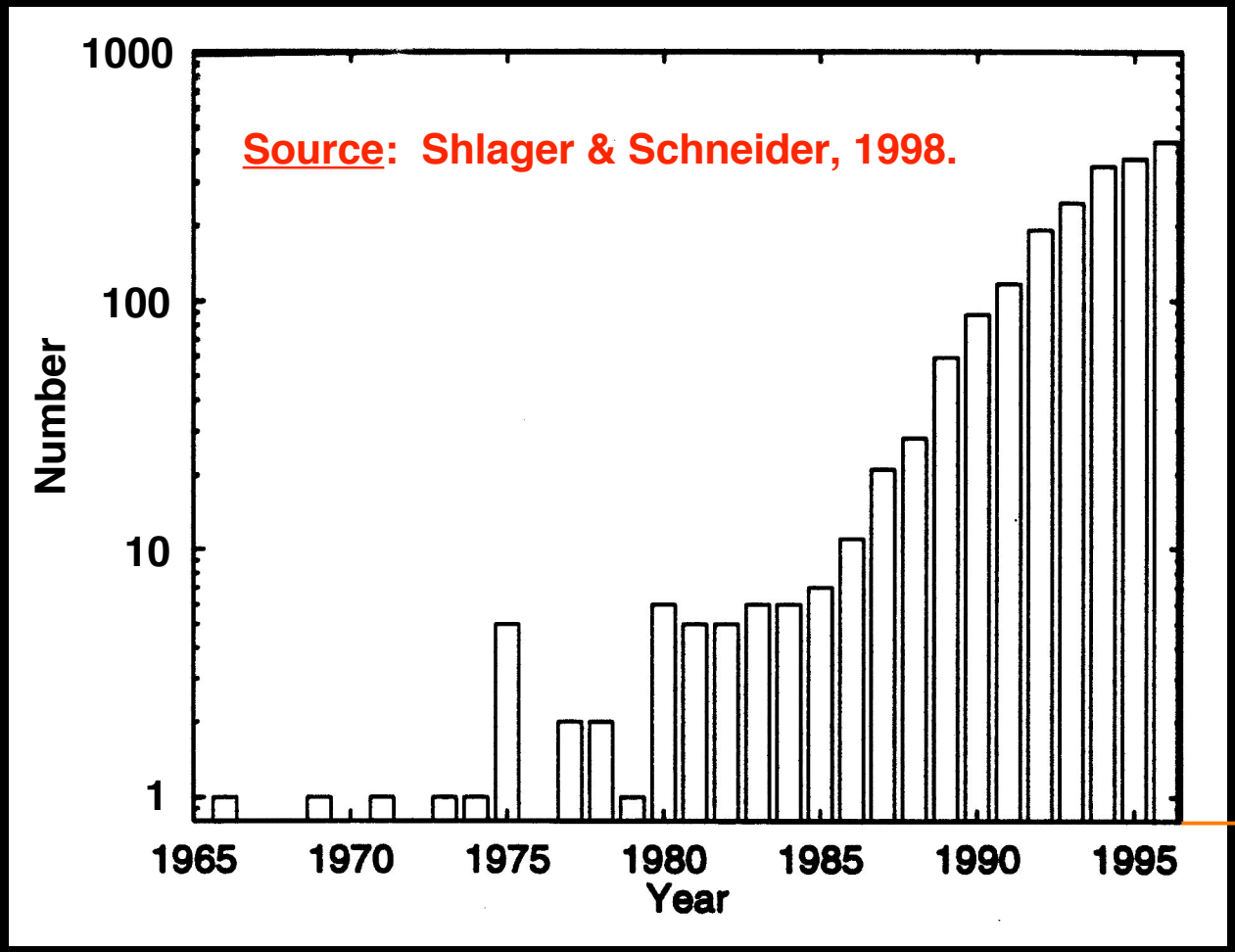

~ 1800

2005

Estimate based on ISI Web of Science topic search.

FDTD Software (as listed in Wikipedia)

Free software / open-source software FDTD projects (4):

- Meep (MIT) ・ (Geo-) Radar FDTD ・ Gfdtd ・ bigboy

Freeware / closed-source FDTD projects (3):

- EMP3 Field Precision ・ EM Explorer ・ GprMax

Commercial / proprietary FDTD software vendors (27):

- Acceleware ・ APLAC ・ Apollo Photonics ・ Applied Simulation Technology
- CFDRC ・ Computer and Communication Unlimited ・ Cray LC ・ CrystalWave
- CST ・ Electro Magnetic Applications ・ Emagware ・ EM Photonics ・ Empire
- EMS Plus ・ ETHZ ・ Lumerical Solutions ・ Nonlinear Control Strategies
- Optiwave ・ Photon Design ・ QuickWave ・ Remcom ・ RM Associates
- Rsoft ・ SEMCAD ・ Taflove-Hagness book ・ Vector Fields ・ Zeland

My First Paper: *IEEE Trans. Microwave Theory & Techniques*, Aug. 1975

Numerical Solution of Steady-State Electromagnetic Scattering Problems Using the Time-Dependent Maxwell's Equations

ALLEN TAFLOVE AND MORRIS E. BRODWIN, SENIOR MEMBER, IEEE

***Abstract*—A numerical method is described for the solution of the electromagnetic fields within an arbitrary dielectric scatterer of the order of one wavelength in diameter. The method treats the irradiation of the scatterer as an initial value problem. At $t = 0$, a plane-wave source of frequency f is assumed to be turned on. The diffraction of waves from this source is modeled by repeatedly solving a finite-difference analog of the time-dependent Maxwell's equations. Time stepping is continued until sinusoidual steady-state field values are observed at all points within the scatterer. The envelope of the standing wave is taken as the steady-state scattered field. As an example of this method, the computed results for a dielectric cylinder scatterer are presented. An error of less than ±10 percent in locating and evaluating the standing-wave peaks within the cylinder is achieved for a program execution time of 1 min. The extension of this method to the solution of the fields within three-dimensional dielectric scatterers is outlined.**

microwaves upon living tissue. Exact analytical solutions are obtained only for simple scatterers like the sphere and the circular cylinder, which may be solved using separation of variables. For complicated scatterers like most body organs, we must resort to some numerical method if an accurate model is to be examined.

The computer techniques relevant to this problem that have appeared in the literature may be called, as a class, frequency-domain methods. These methods are based upon the assumption of an exp $(j2\pi ft)$ time dependence in the fundamental Maxwell's equations. In general, methods of this type derive a set of linear equations for either field variables or field expansion coefficients, and then solve the linear system with a suitable matrix-inversion scheme.

"FDTD" Coined: *IEEE Trans. Electromagnetic Compatibility*, Aug. 1980

IEEE TRANSACTIONS ON ELECTROMAGNETIC COMPATIBILITY, VOL. EMC-22, NO. 3, AUGUST 1980

Application of the Finite-Difference Time-Domain Method to Sinusoidal Steady-State Electromagnetic-Penetration Problems

ALLEN TAFLOVE, MEMBER, IEEE

Abstract—**A numerical method for predicting the sinusoidal steady-state electromagnetic fields penetrating an arbitrary dielectric or conducting body is described here. The method employs the finite-difference time-domain (FD–TD) solution of Maxwell's curl equations implemented on a cubic-unit-cell space lattice. Small air-dielectric loss factors are introduced to improve the lattice truncation conditions and to accelerate convergence of cavity interior fields to the sinusoidal steady state. This method is evaluated with comparison to classical theory, method-of-moment frequency-domain numerical theory, and experimental results via application to a dielectric sphere and a cylindrical metal cavity with an aperture. Results are also given for a missile-like cavity with two different types of apertures illuminated by an axial-incidence plane wave.**

Key Words—**Finite-difference, time-domain, steady-state, plane wave, electromagnetic penetration, apertures, dielectric sphere, cylindrical metal cavity, missile-like cavity.**

modeling approaches. First, it is simple to implement for complicated metal/dielectric structures because arbitrary electrical parameters can be assigned to each lattice cell using a data card deck. Second, its computer memory and running time requirement is not prohibitive for many complex structures of interest. In recent work, the FD–TD method has been shown capable of accurately solving for hundreds of thousands of unknown field components within a few minutes on an array-processing computer. Consistently, a ±1-dB accuracy relative to known analytical and experimental bench marks has been achieved for a variety of dielectric and metal geometries.

The objective of present work is to evaluate the suitability of the FD–TD method to determine the amount of elec-

Some Major Technical Paths Since Yee

- Absorbing boundary conditions
- Numerical dispersion
- Numerical stability
- Conforming grids
- Digital signal processing
- Dispersive and nonlinear materials
- Multiphysics

Some Major Technical Paths Since Yee

- Absorbing boundary conditions
  - Analytical
    - One-way wave equations (Engquist & Majda, *Math. Comp.*, 1977)
    - Outgoing wave annihilators (Bayliss & Turkel, *Com. Pure Appl. Math.*, 1980)
    - Space-time extrapolation (Liao et al., *Scientia Sinica A*, 1984)
  - Perfectly matched layer — PML
    - Split field (Berenger, *JCP*, 1994)
    - Uniaxial (Sacks et al, *IEEE AP*, 1995)
    - Complex frequency-shifted (Kuzuoglu & Mittra, *IEEE MGWL*, 1996)

Some Major Technical Paths Since Yee

- Numerical dispersion
  - Schneider & Wagner analysis, *IEEE MGWL*, 1999
  - High-order space differences (many workers)
  - Multi-resolution time-domain — MRTD (Krumpholz & Katehi, *IEEE MTT*, 1996)
  - Pseudospectral time-domain — PSTD (Q. H. Liu, *1997 IEEE AP-S Symp.*)

Some Major Technical Paths Since Yee

- Numerical stability / time-stepping
  - Taflove & Brodwin analysis, *IEEE MTT*, 1975
  - Alternating-direction implicit (ADI) techniques (Namiki, *IEEE MTT,* 1999; Zheng et al, *IEEE MTT*, 2000)
  - Matrix-exponential methods (De Raedt et al., *IEEE AP,* 2003)
  - Nondissipative high-order symplectic techniques (Hirono et al, *IEEE MGWL*, 1997)

Some Major Technical Paths Since Yee

- Conforming grids / subgrids
  - Locally conforming contour path (Jurgens et al, *IEEE AP*, 1992; Dey & Mittra, *IEEE MGWL*, 1997; Yu & Mittra, 2001)
  - Globally conforming (Shankar et al., *Electromagnetics*, 1990; Madsen & Ziolkowski, *Electromagnetics*, 1990)
  - Stable hybrid FETD / FDTD (Rylander & Bondeson, *Comput. Phys. Comm.*, 2000)
  - Stable multiply-nested subgrids (Chavannes, 2005)
  - Quadratic convergence subpixel smoothing (Farjadpour et al, *Optics Lett.,* 2006)

Some Major Technical Paths Since Yee

- Digital signal processing
  - Near-to-far-field transformation (Umashankar & Taflove, *IEEE EMC*, 1982, 1983)
  - Impulse response extrapolation; extraction of resonances (possibly nearly degenerate)
    - Prony's method, linear prediction (many workers)
    - Padé approximation with Baker's algorithm (Guo et al, *IEEE MWCL*, 2001)
    - Filter-diagonalization method (Johnson et al, *Applied Physics Lett.*, 2001)

Some Major Technical Paths Since Yee

- Linear dispersive materials
  - Single-pole Debye and Lorentz dispersions (Kashiwa & Fukai, *MOT Lett.*, 1990; Joseph et al, *Optics Lett.*, 1991; Luebbers et al, *IEEE AP*, 1992, '93, '96)
  - Arbitrary combinations of Debye, Lorentz, and Drude dispersions modeled using recursive convolutions, auxiliary differential equations, or Z-transforms (many workers)
  - High-order rational polynomial functions of frequency (Grande et al, *IEEE AP Intl. Symp.*, 2006)

Some Major Technical Paths Since Yee

- Nonlinear materials
  - Kerr and Raman nonlinearities modeled for scalar temporal and spatial solitons (Goorjian & Taflove, *Optics Lett.*, 1992; Joseph & Taflove, *IEEE PTL*, 1994)
  - Efficient reformulation allowing a multipole Sellmeier linear dispersion to be modeled along with Kerr and Raman nonlinearities (S. Nakamura et al, *IEICE Trans. Electron.*, 2003)
  - Multipole Sellmeier linear dispersion + Kerr and Raman nonlinearities modeled for vector spatial solitons (Greene & Taflove, *Optics Express*, 2006)

Some Major Technical Paths Since Yee

- Multiphysics coupling to Maxwell's equations
  - Charge generation,recombination, and transport in semiconductors (El-Ghazaly et al., *IEEE MTT*, 1990)
  - Electron transitions between multiple energy levels of atoms, modeling pumping, emission, and stimulated-emission processes
    - Two-level atoms (Ziolkowski et al., *Phys. Rev. A*, 1995); Nagra & York (*IEEE AP*, 1998)
    - Four-level atoms (Huang, M.S. thesis, 2002); Chang & Taflove, *Optics Express*, 2004)
    - Multi-level atoms (Huang & Ho, *Optics Express*, 2006)

Index-Contrast Waveguides and Cavities

2-D Laterally Coupled Photonic Disk Resonator

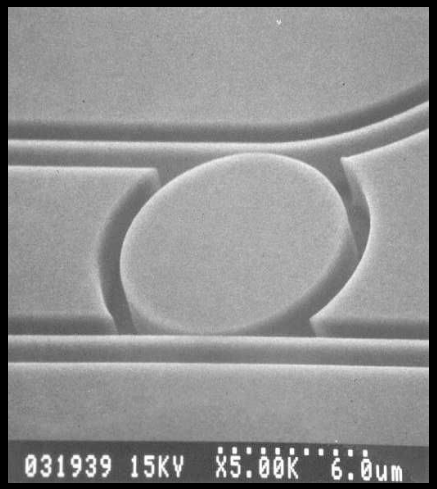

fabricated device

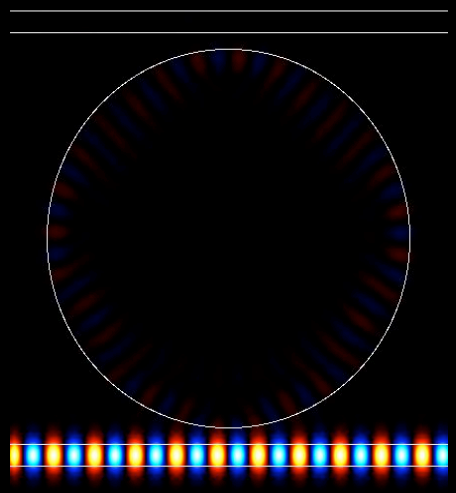

λ = 1.55 μm
(off resonance)

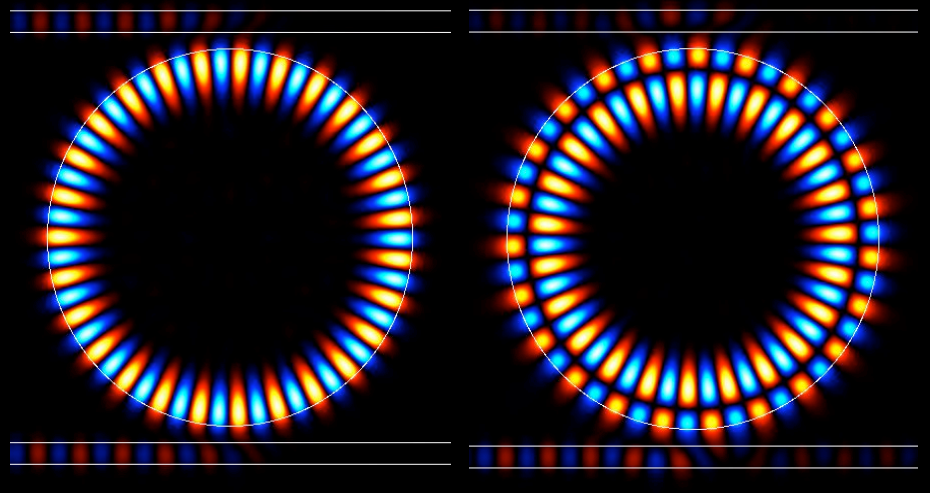

1st- and 2nd-order radial whispering gallery mode resonances

Source: Hagness et al, *IEEE J. Lightwave Tech.*, 1997.

3-D Vertically Coupled Photonic Racetrack

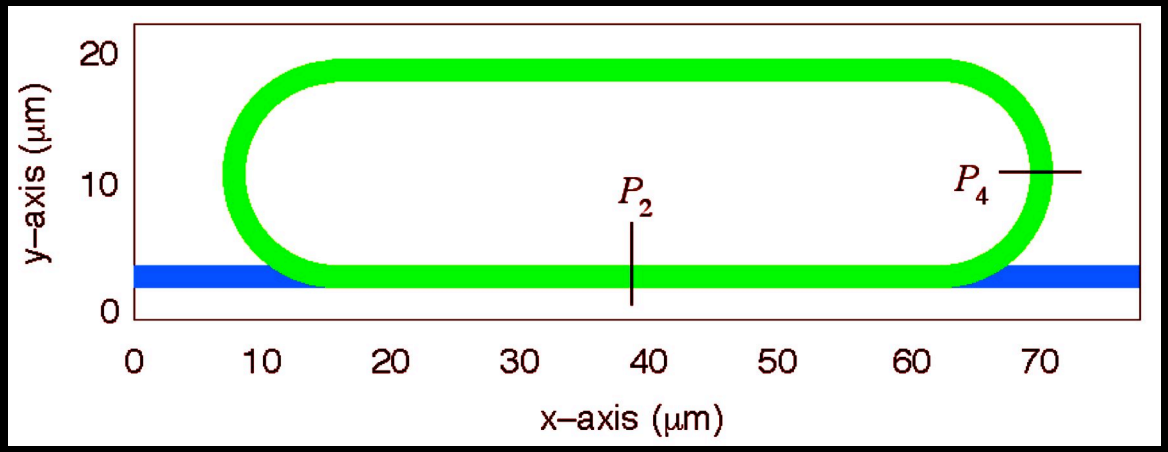

Plan view

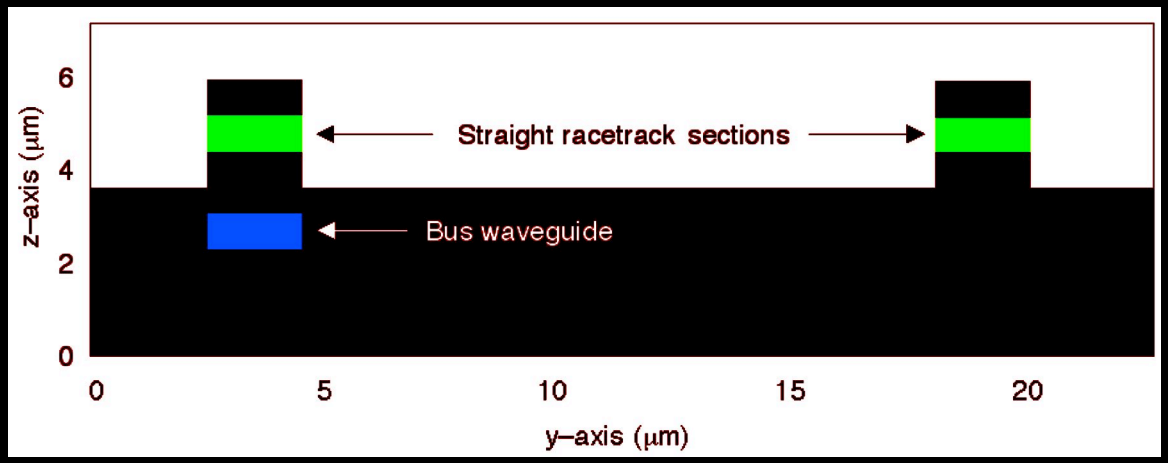

Vertical cross-section

Source: Greene and Taflove, *Optics Letters*, 2003.

Pulse Propagation in Vertically Coupled Racetrack

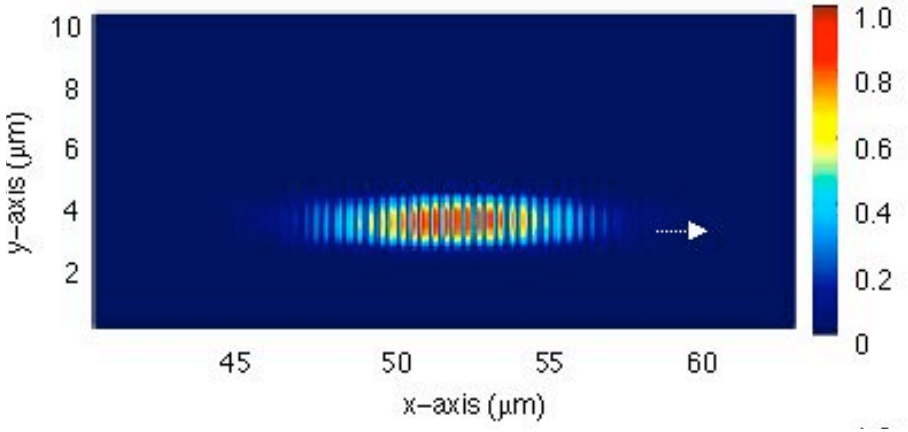

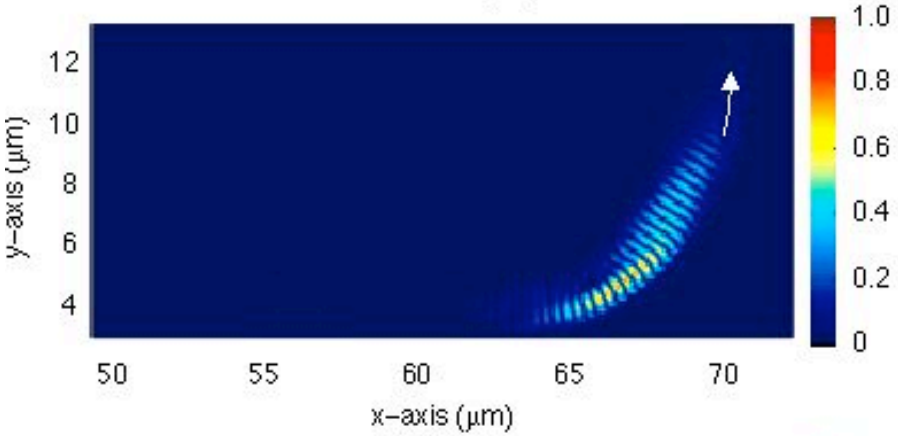

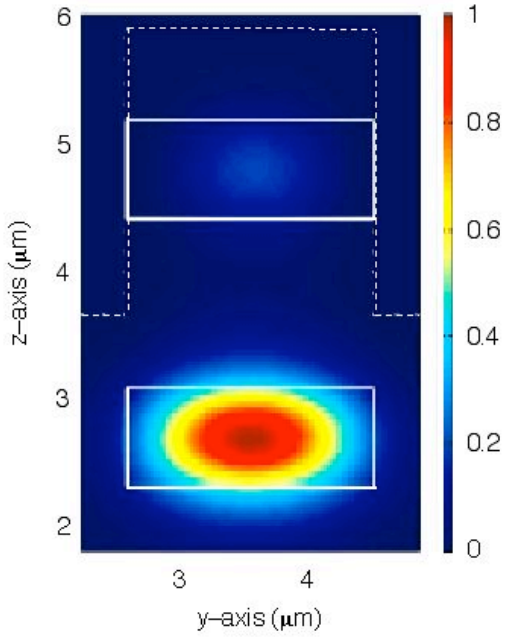

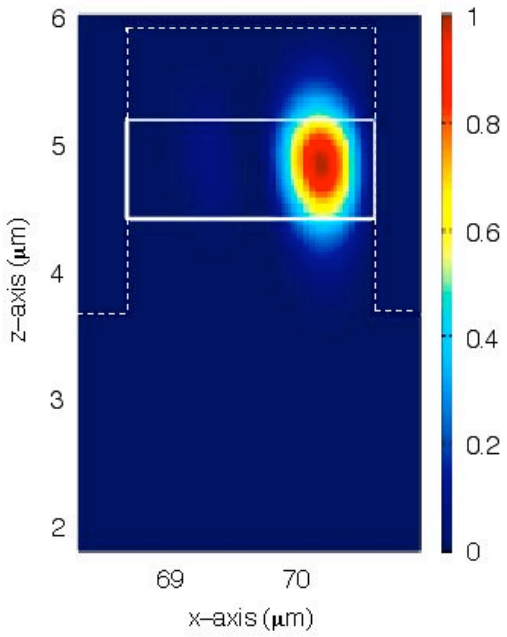

Standing Waves in Convex Dielectric Bodies

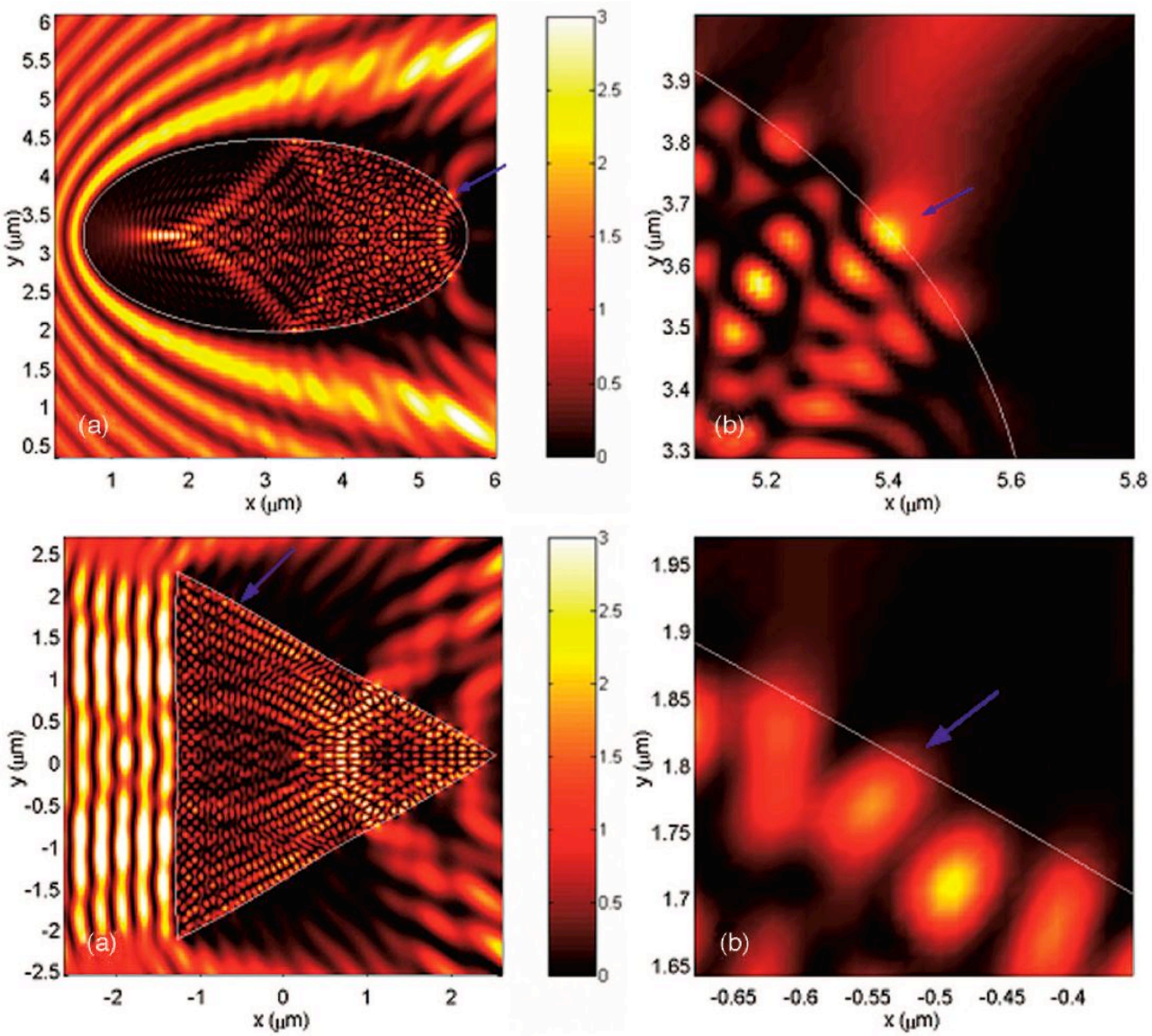

Source: Chen et al, ***Applied Optics***, **Feb. 1, 2006, pp. 633-638.**

Photonic “Nanojet” Exiting a Dielectric Sphere

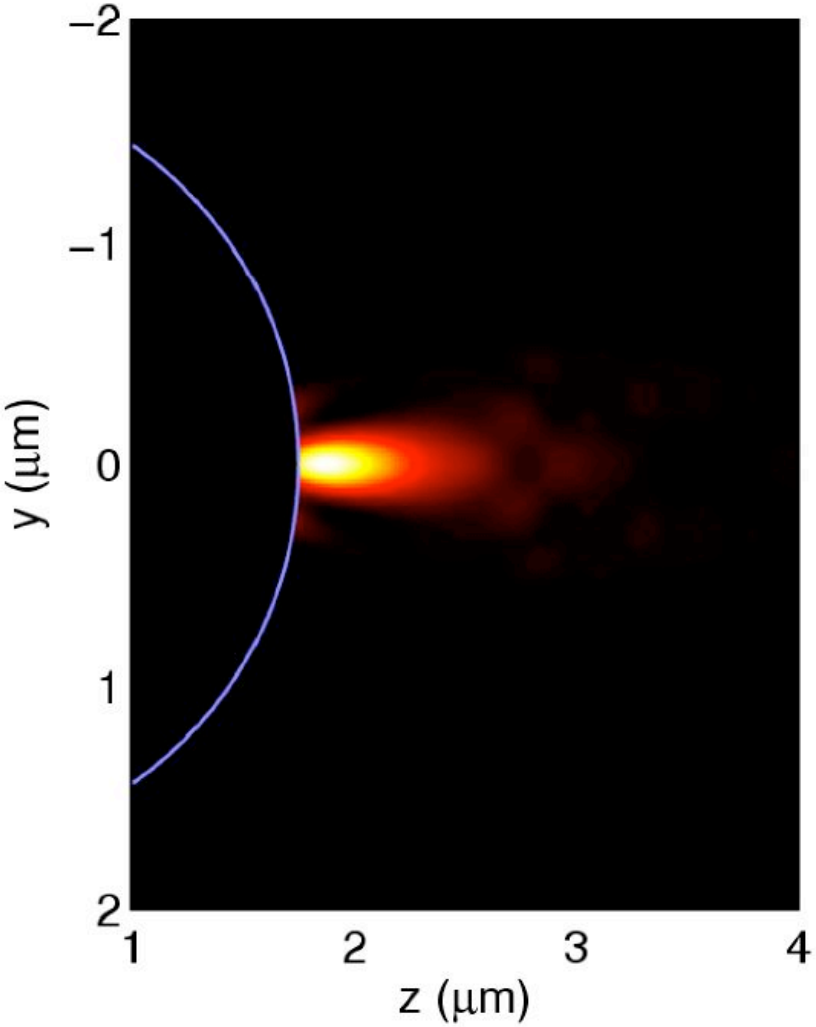

Narrow minimum beamwidths ranging from $0.3\lambda_0$ to $0.5\lambda_0$

Well-collimated over propagation distances of $\sim 1\lambda_0$

Broadband (exist over a wide range of incident λ_0 and refractive indices)

Provide giant enhancements of the backscattering of nanoparticles

Source: Li et al, *Optics Express*, Jan. 24, 2005, pp. 526-533.

20-nm Gold Particle Traversing the Nanojet

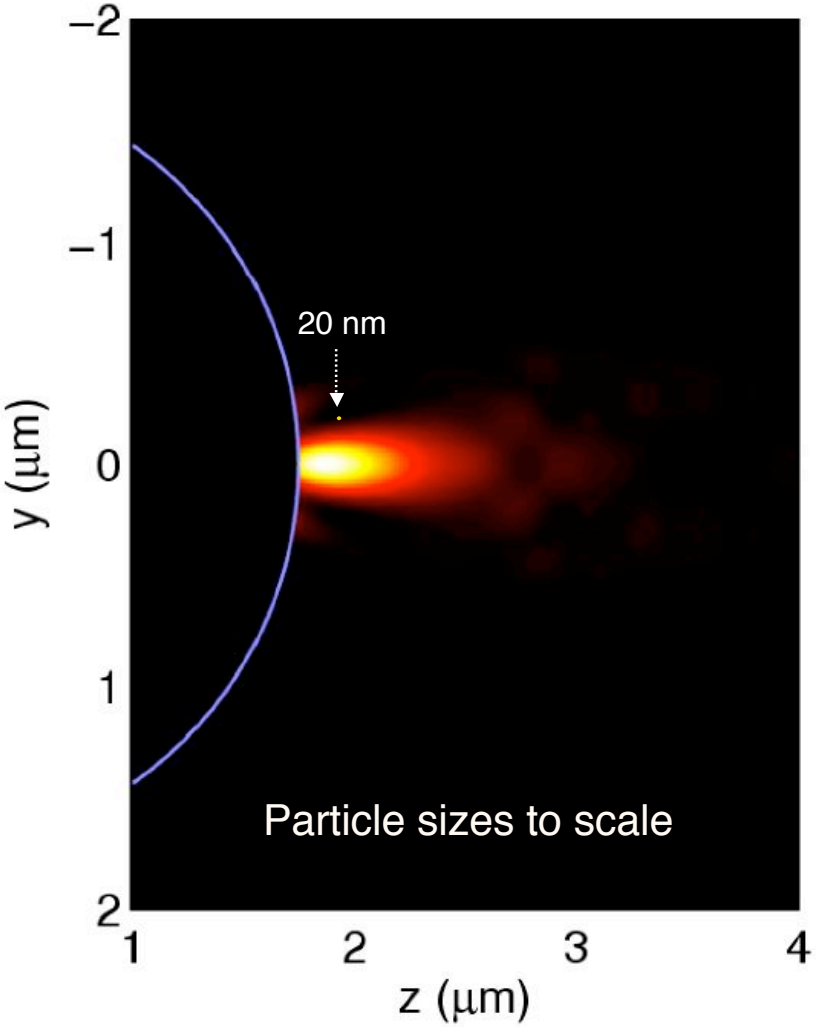

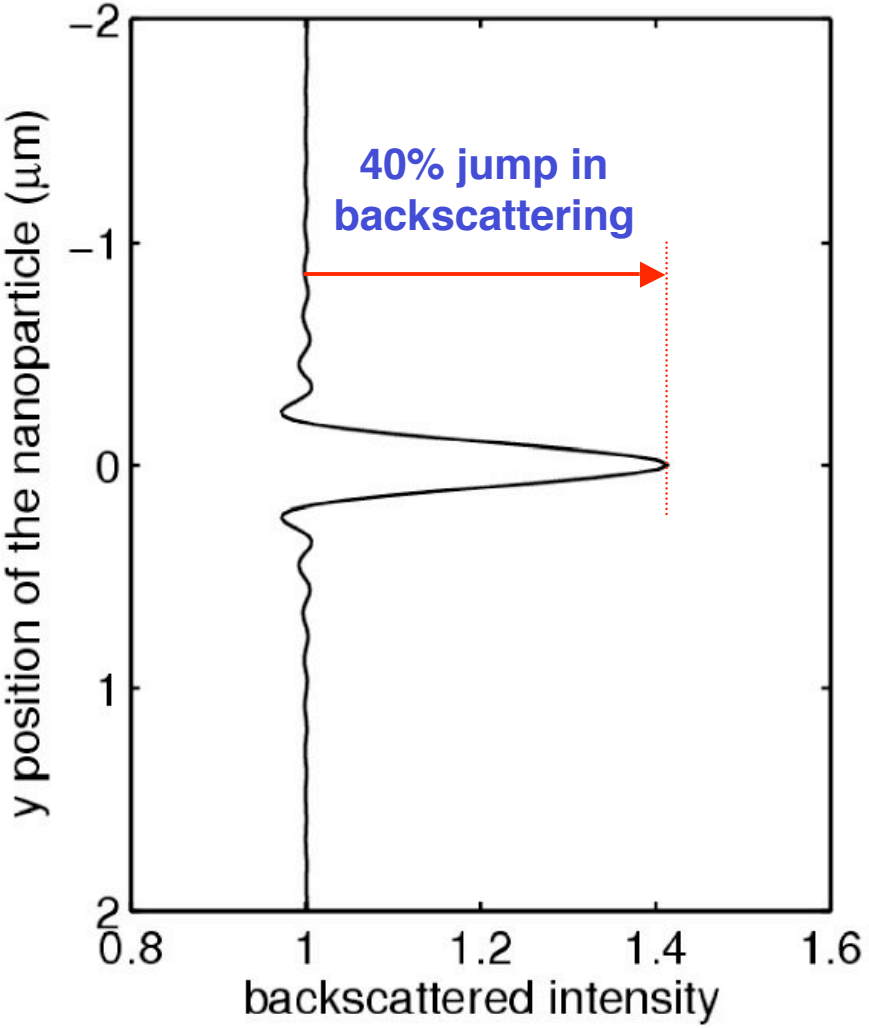

Giant Backscattering Enhancement: Prediction & Validation

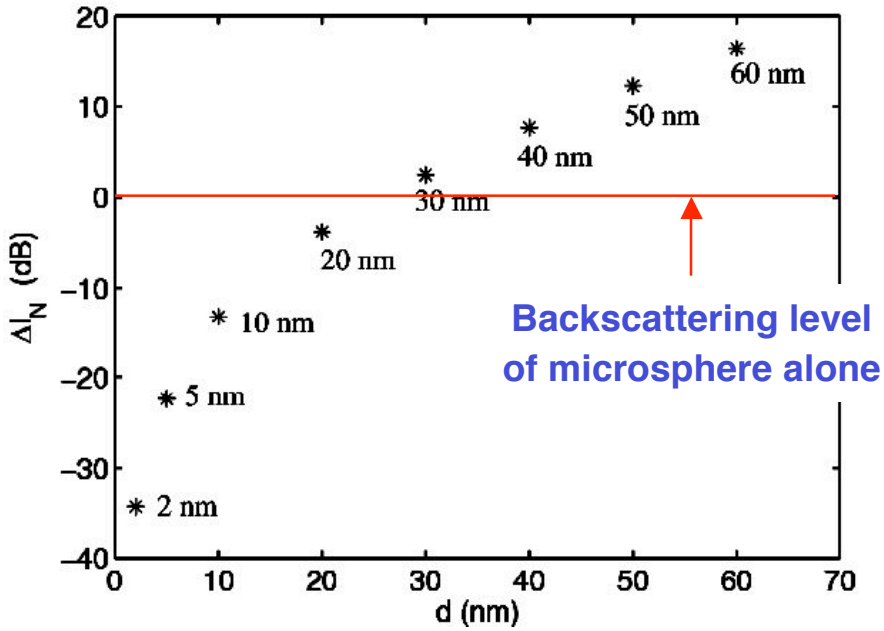

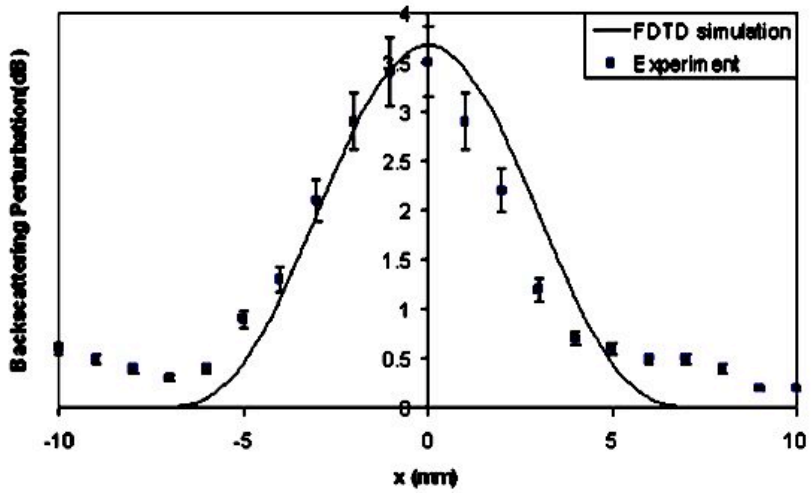

FIG. 5. (Color online) Measured and FDTD-calculated backscattering perturbation caused by the 1 mm metal particle scanned laterally across the microwave jet at a fixed distance z=9 mm from the top surface of the acrylic sphere (log-linear plot).

Source: Li et al, *Optics Express*, Jan. 24, 2005, pp. 526-533.

Source: Heifetz et al, *Applied Physics Lett.* 89, 221118, Nov. 2006.

Photonic Crystal Defect-Mode Waveguides and Cavities

3-D FDTD Bandstructure Calculations Agree With PSNOM Measurements for a Slow-Light Photonic Crystal Structure

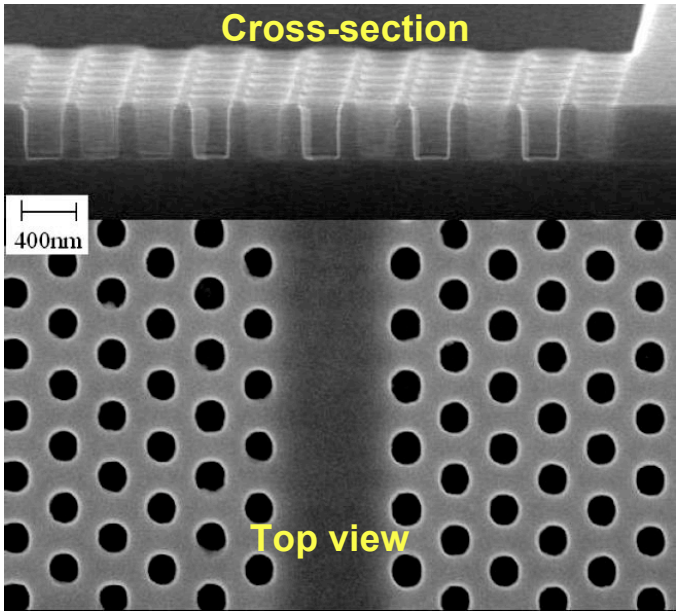

Lattice period = 420 nm;
hole diameter = 235 nm

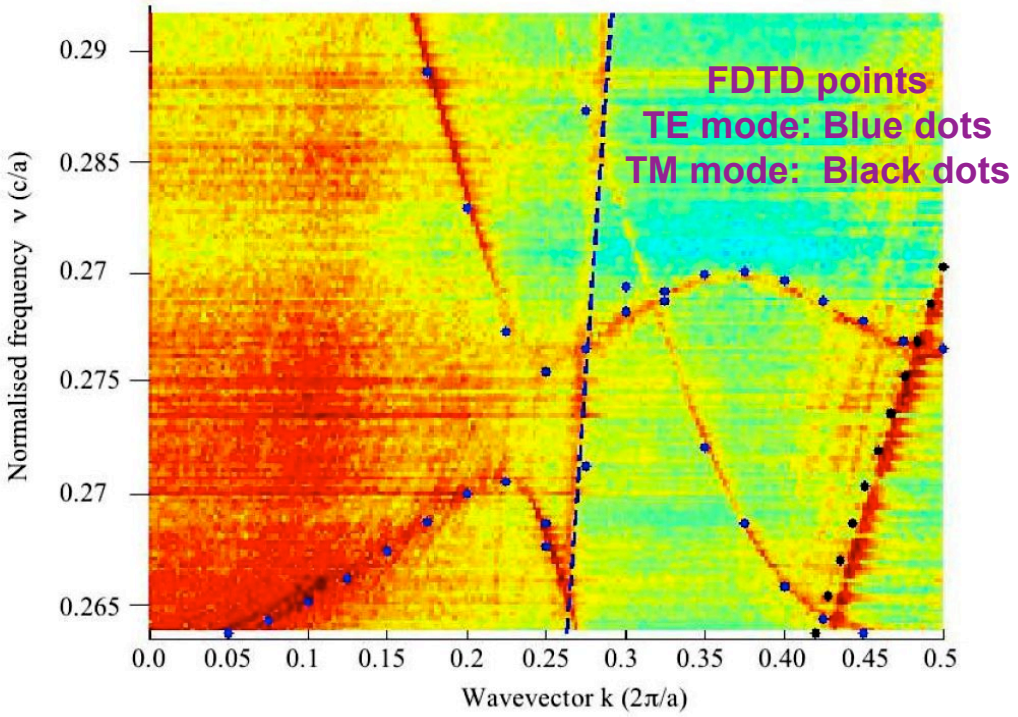

Source: Settle et al., *Optics Express*, Jan. 8, 2007, pp. 219-226.

Wavelength-Dependent Short-Wall Coupler

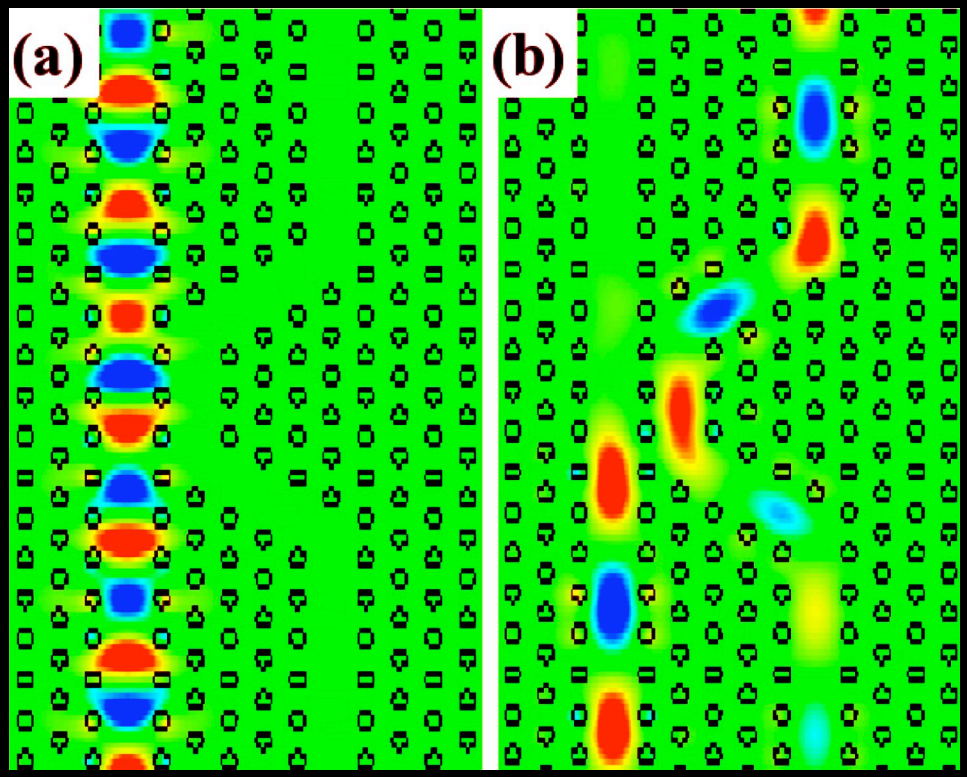

Source: F. Chien et al, *Optics Express*, March 22, 2004.

Photonic Crystal Defect-Mode Cavities

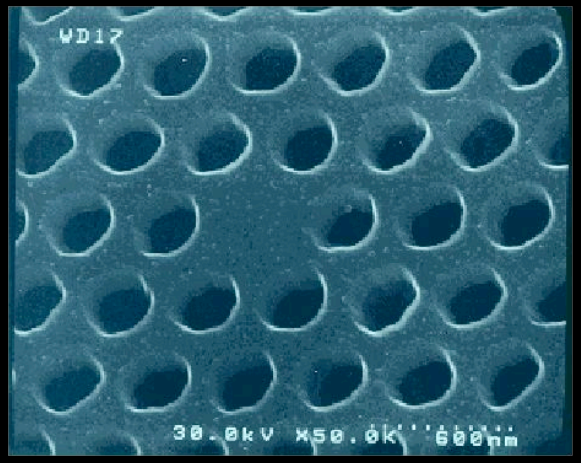

Fabricated device:
membrane microresonator
in InGaAsP

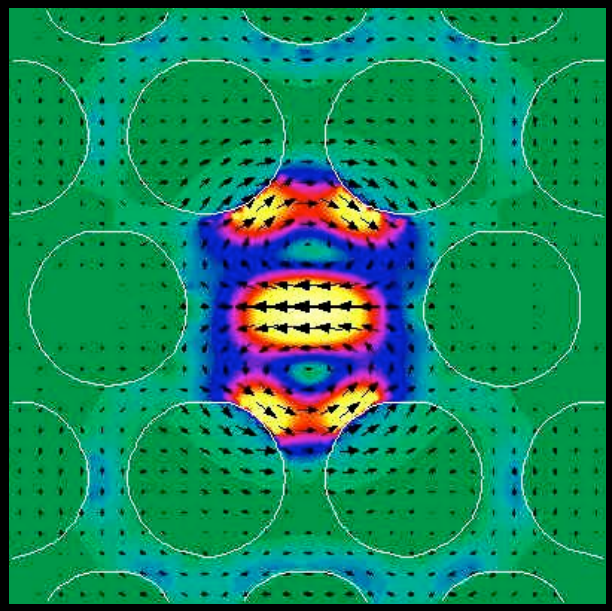

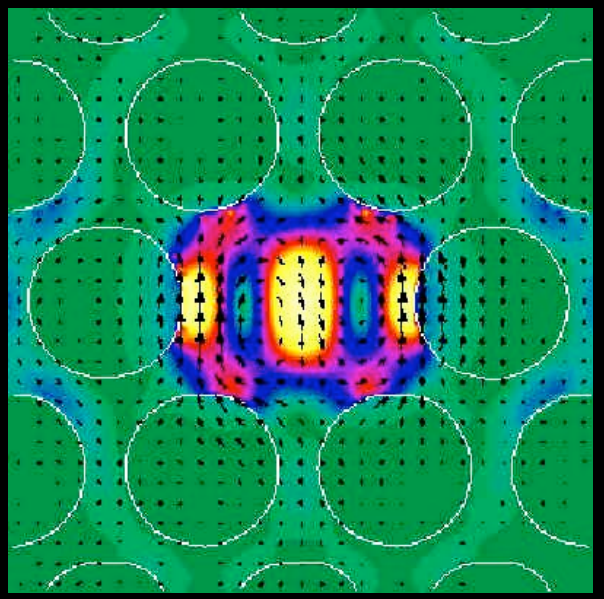

Images of degenerate microcavity modes in
2-D thin-film photonic crystal defect cavities

Source: E. Yablonovitch

Photonic Crystal Defect-Mode Laser Cavities

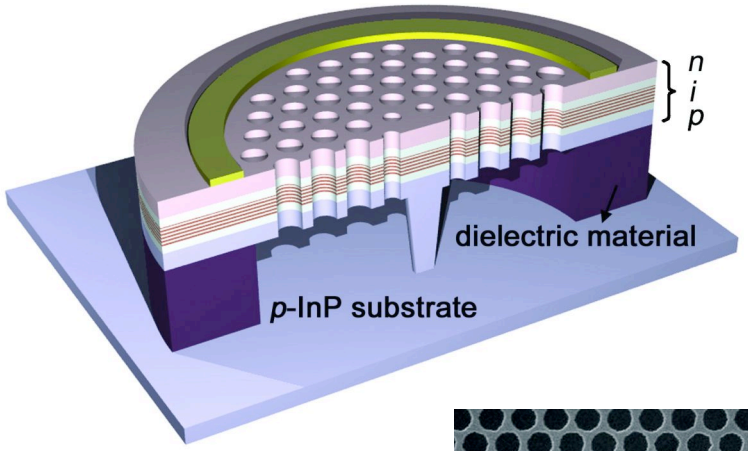

Schematic view

Electrically driven, single-mode, low-threshold-current photonic crystal microlaser operating at room temperature.

Source: Park et al., *Science*, Sept. 3, 2004, pp. 1444–1447.

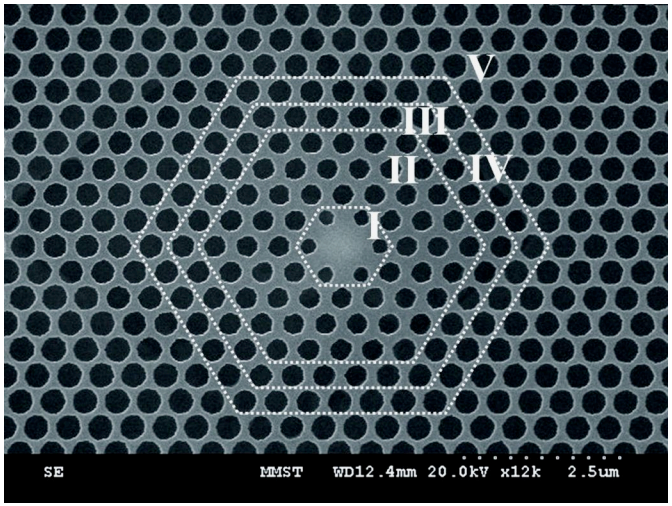

Top view of fabricated sample

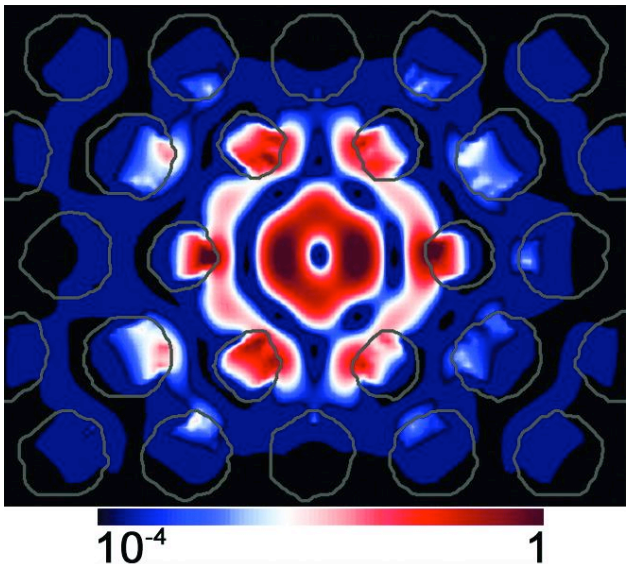

E-field intensity of monopole mode (log scale)

Plasmonics

Prism-Coupled Surface Plasmon Polariton on Both Sides of a 65-nm-thick Silver Film

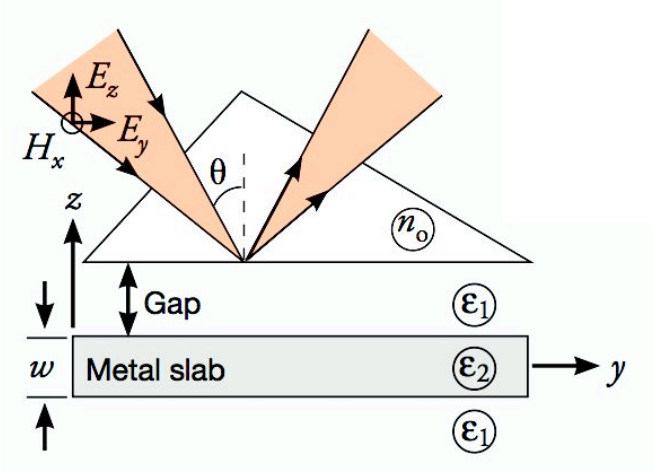

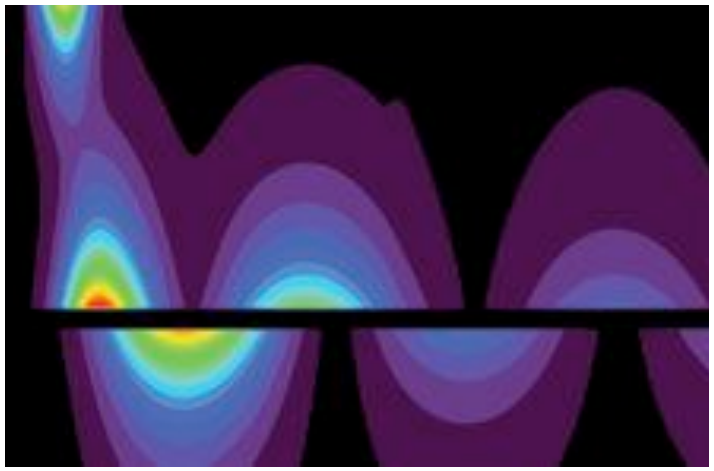

E_y distribution

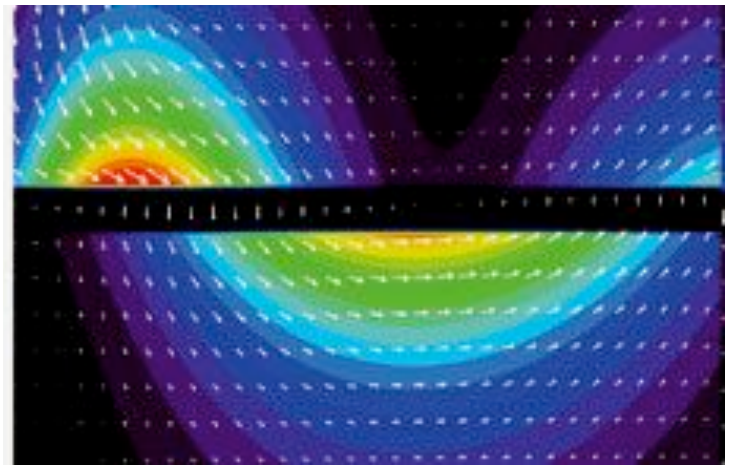

Poynting vector distribution

Source: M. Mansuripur et al., *Optics & Photonics News*, April 2007, pp. 44-49.

Plasmon-Enhanced Transmission Through a 200-nm-diameter Hole in a 100-nm-thick Gold Film

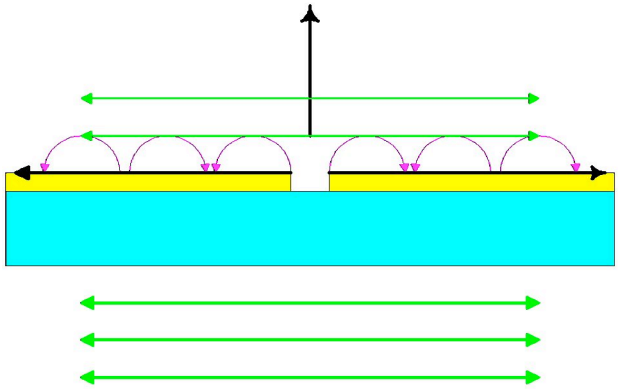

Incident wavelength = 532 nm
Normal incidence

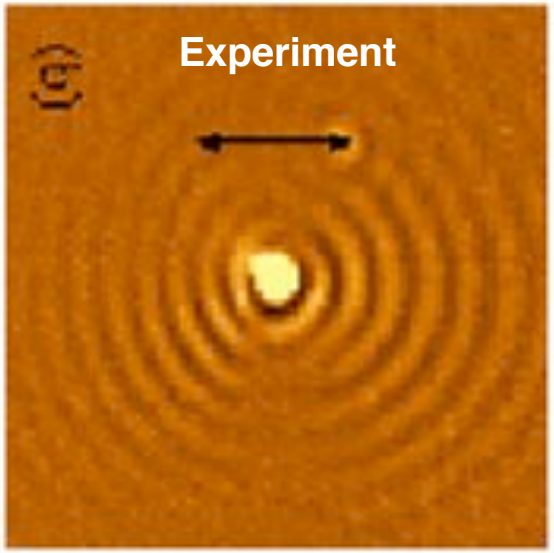

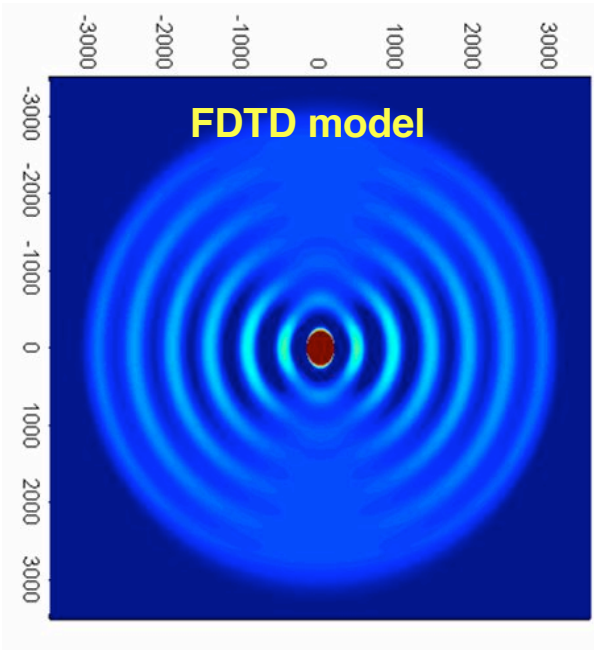

Source: L. Yin et al., *Applied Physics Letters* 85, 467 (2004)

Focusing Plasmonic Lens

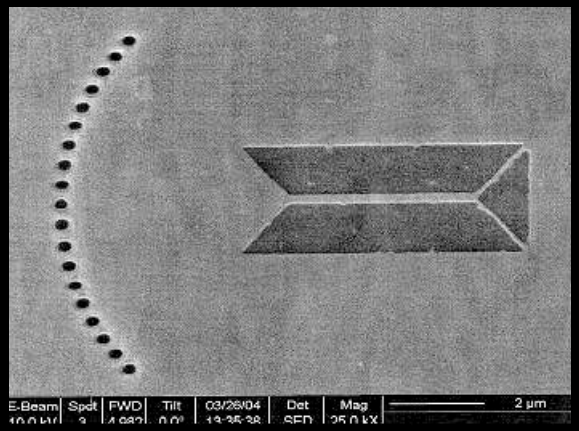

SEM photo

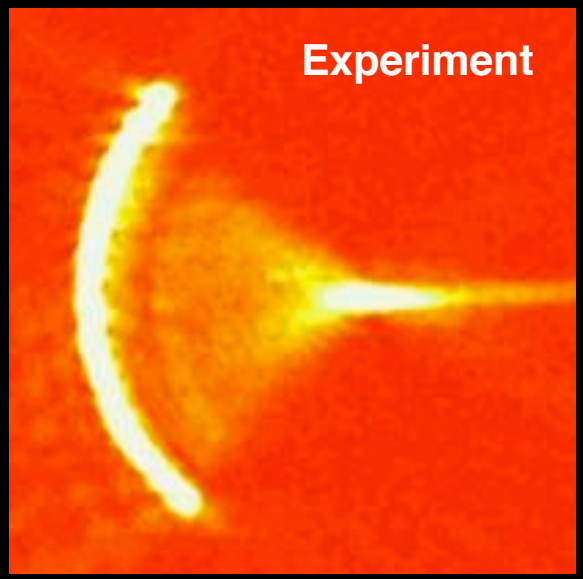

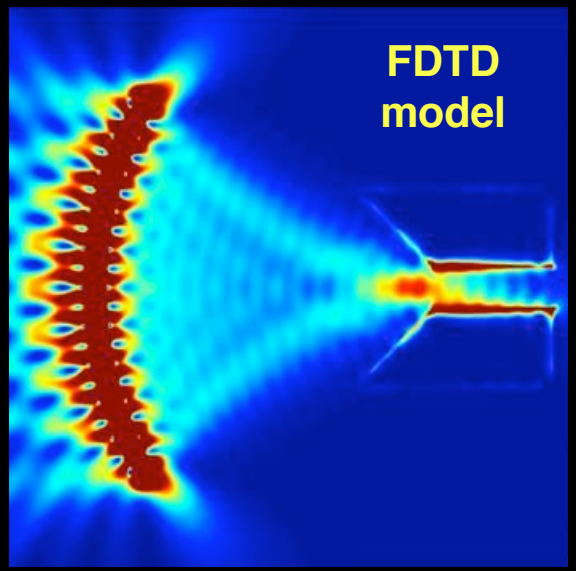

Source (left and bottom left images):
L. Yin et al., *Nano Letters* 5, 1399 (2005).

Source (bottom right image): S-H. Chang

Waveguide Comprised of Gold Nanoparticles

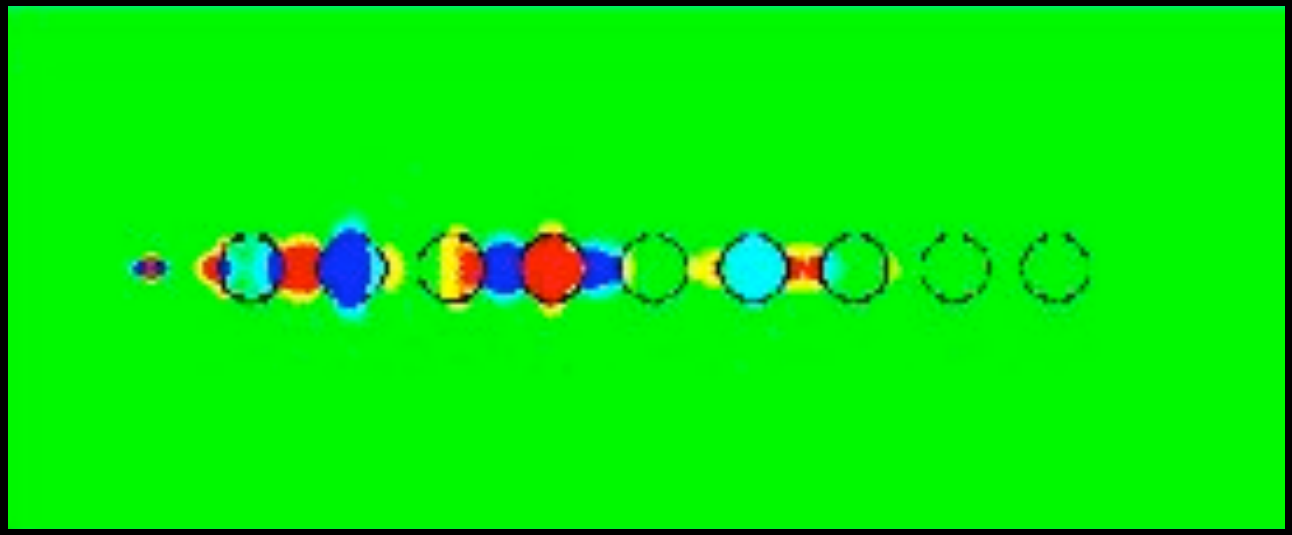

Source: Harry Atwater, Caltech
http://daedalus.caltech.edu/research/plasmonics.php

“Invisibility” Cloak Based on a Plasmonic Material

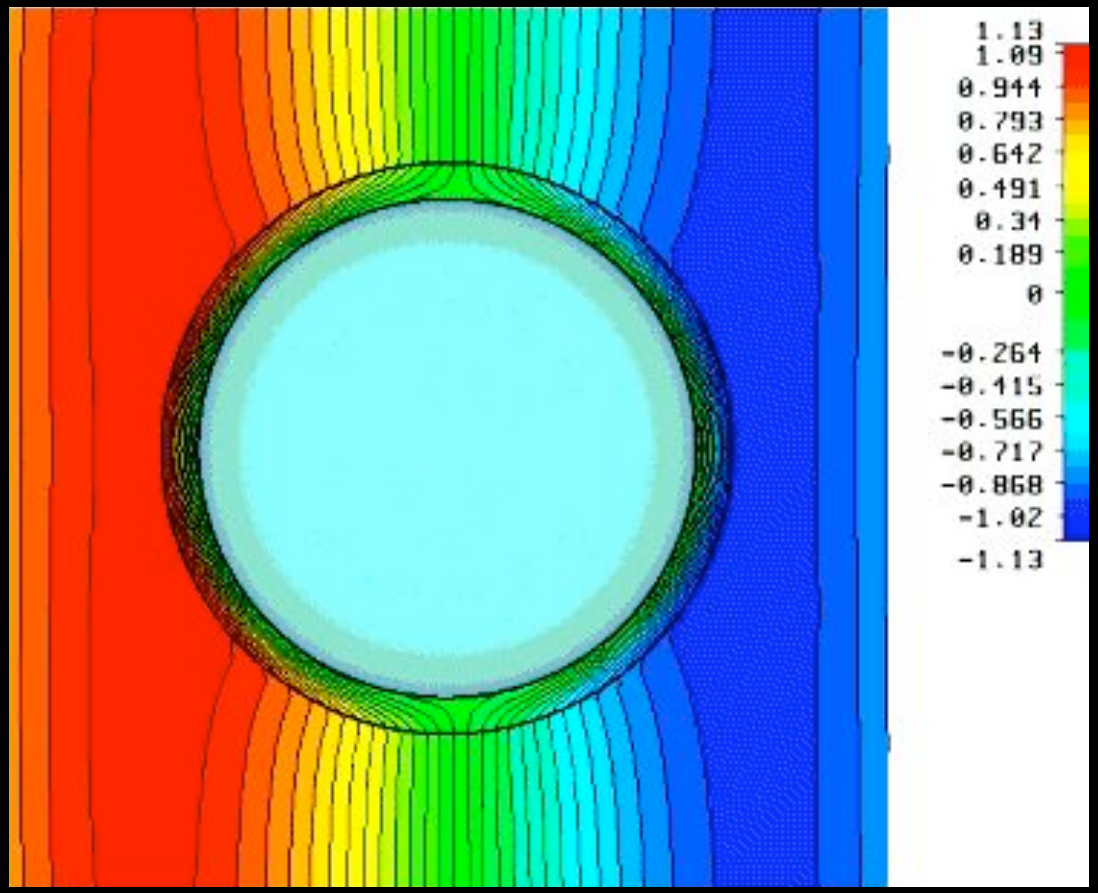

Snapshot of the time-domain E-field distribution in the H-plane. The E-field is orthogonal to the plane of the figure.

Source: Alu and Engheta, *Optics Express*, March 19, 2007, pp. 3318-3332.

Macroscopic Nonlinearities Yielding Spatial Solitons and Switching Action

“Braided” Co-Phased Spatial Solitons in Glass

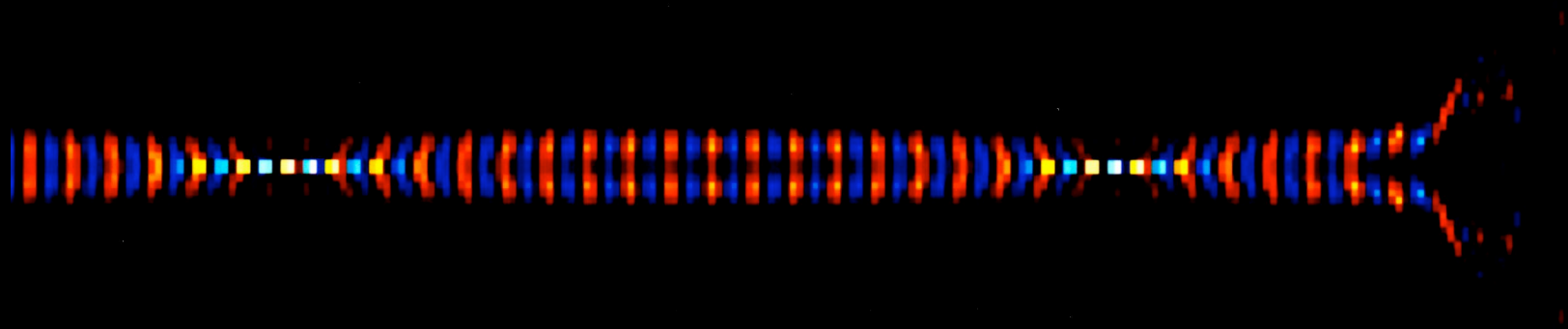

Source: Joseph and Taflove, *IEEE Photonics Technology Lett.*, 1994.

Vector Spatial Solitons Scattered by Subwavelength Air Holes

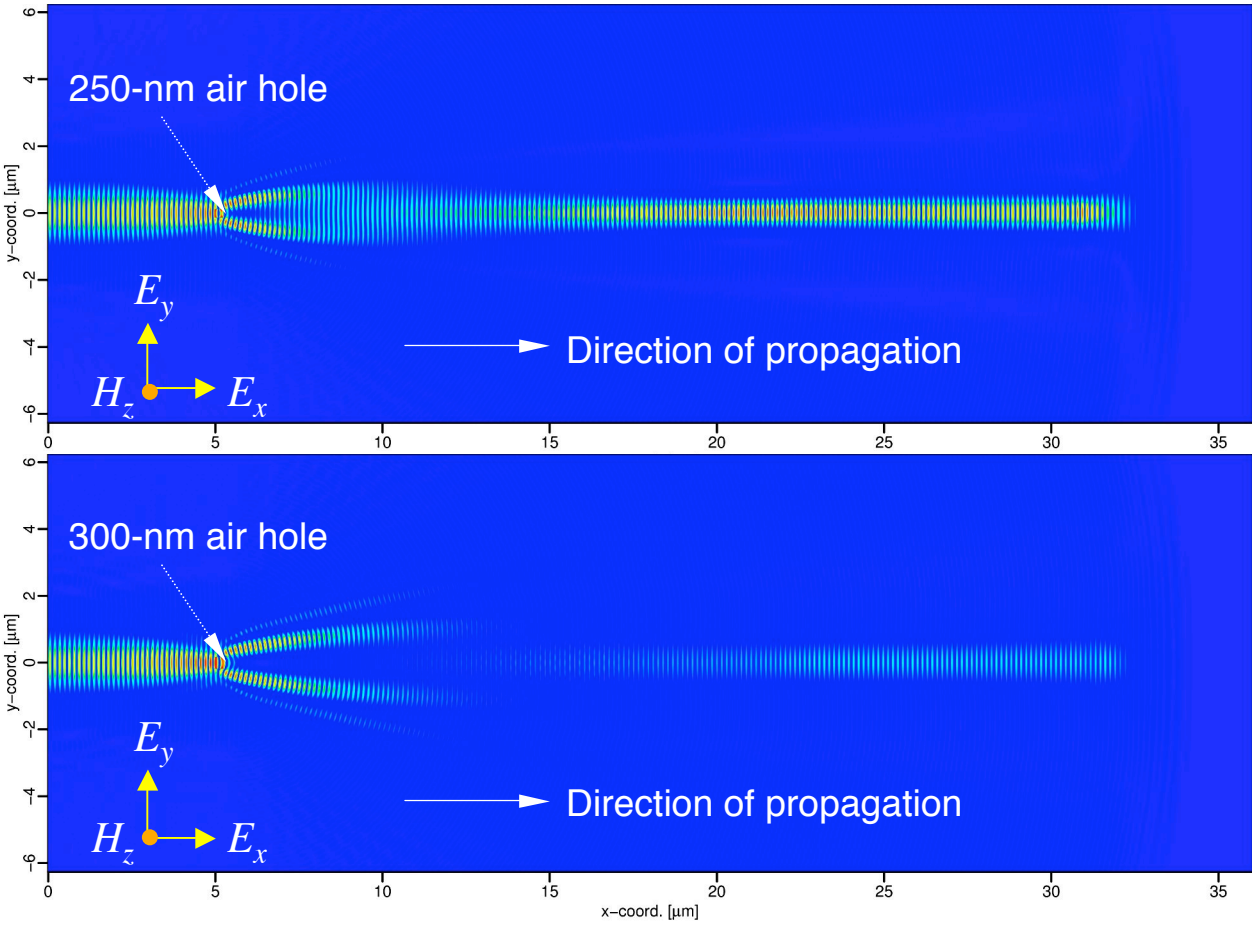

Here, glass is modeled for realistic 3-pole Sellmeier linear dispersions + Kerr + Raman nonlinearities.

The spatial solitons are +x-directed and have the field components H_z, E_x, and E_y.

Source: Greene and Taflove, work in progress.

All-Optical Photonic Crystal Cross-Waveguide Switch

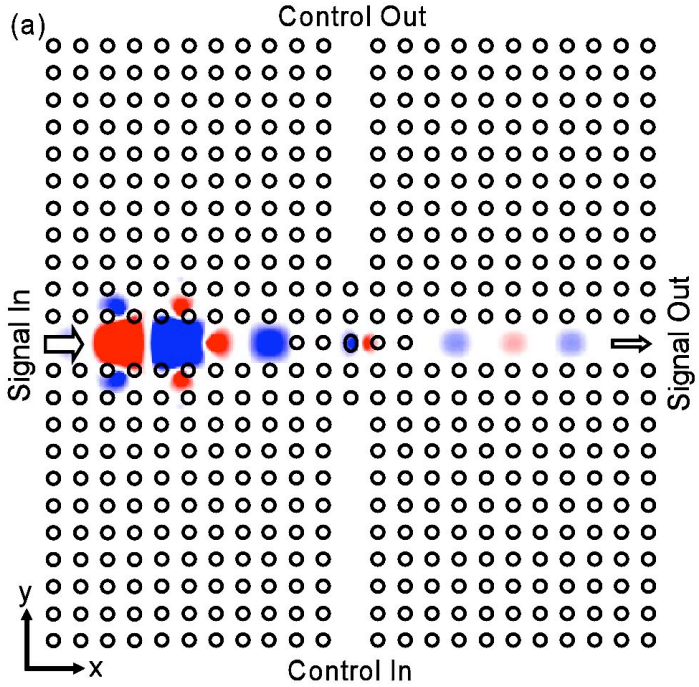

Control input is absent, yielding low signal output

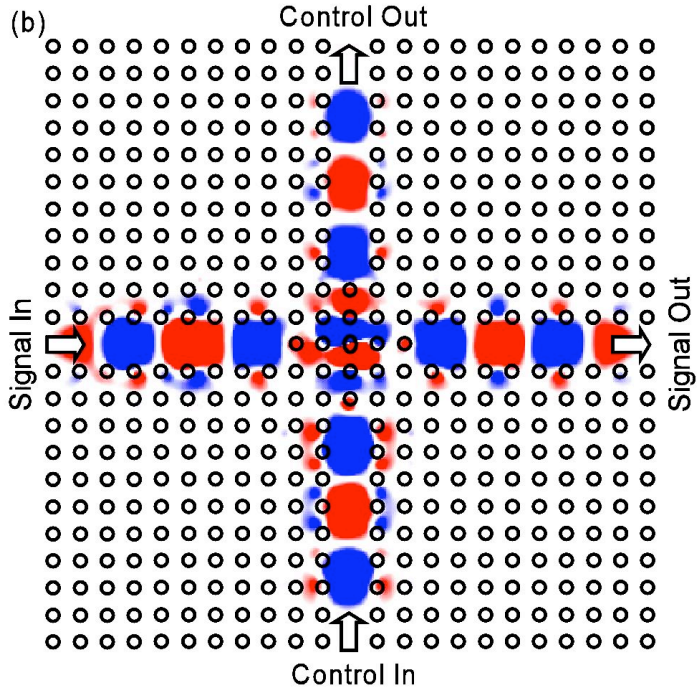

Control input is present, yielding high signal output

Source: Yanik et al., *Optics Lett.*, 2003, pp. 2506–2508.

Semiclassical Models of Lasers

Four-Level, Two-Electron Model for ZnO

$$\frac{d^2 P_a}{dt^2} + \gamma_a \frac{dP_a}{dt} + \omega_a^2 P_a = k_a \left[N_3 - N_0 \right] E$$

$$\frac{d^2 P_b}{dt^2} + \gamma_b \frac{dP_b}{dt} + \omega_b^2 P_b = k_b \left[N_2 - N_1 \right] E$$

$$\frac{dN_3}{dt} = -\frac{N_3(1-N_2)}{\tau_{32}} - \frac{N_3(1-N_0)}{\tau_{30}} + \frac{1}{\hbar\omega_a} E \cdot \frac{dP_a}{dt}$$

$$\frac{dN_2}{dt} = \frac{N_3(1-N_2)}{\tau_{32}} - \frac{N_2(1-N_1)}{\tau_{21}} + \frac{1}{\hbar\omega_b} E \cdot \frac{dP_b}{dt}$$

$$\frac{dN_1}{dt} = \frac{N_2(1-N_1)}{\tau_{21}} - \frac{N_1(1-N_0)}{\tau_{10}} - \frac{1}{\hbar\omega_b} E \cdot \frac{dP_b}{dt}$$

$$\frac{dN_0}{dt} = \frac{N_3(1-N_0)}{\tau_{30}} + \frac{N_1(1-N_0)}{\tau_{10}} - \frac{1}{\hbar\omega_a} E \cdot \frac{dP_a}{dt}$$

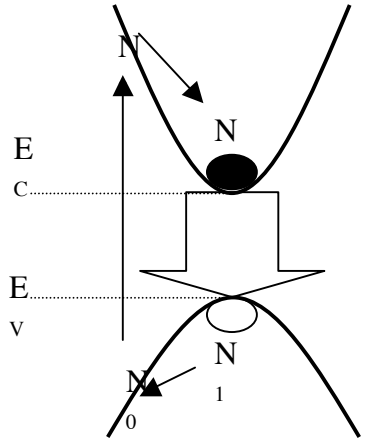

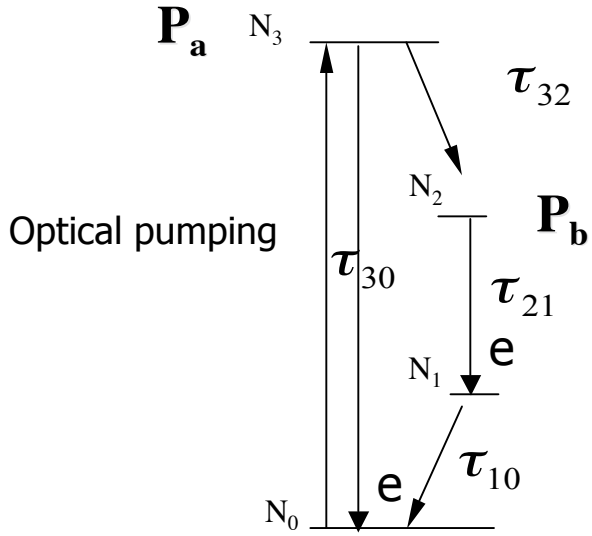

Optical pumping

Source: **Chang and Taflove, *Optics Express*, 2004.**

1-D Four-Level Two-Electron Model of Pumping, Population Inversion, and Lasing

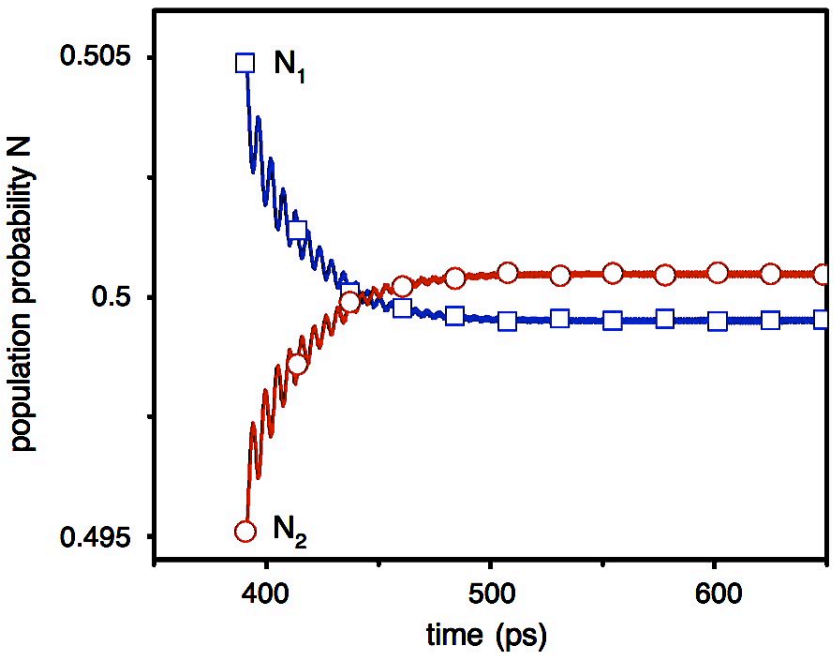

Electron population density probability showing the inversion between Levels 1 and 2

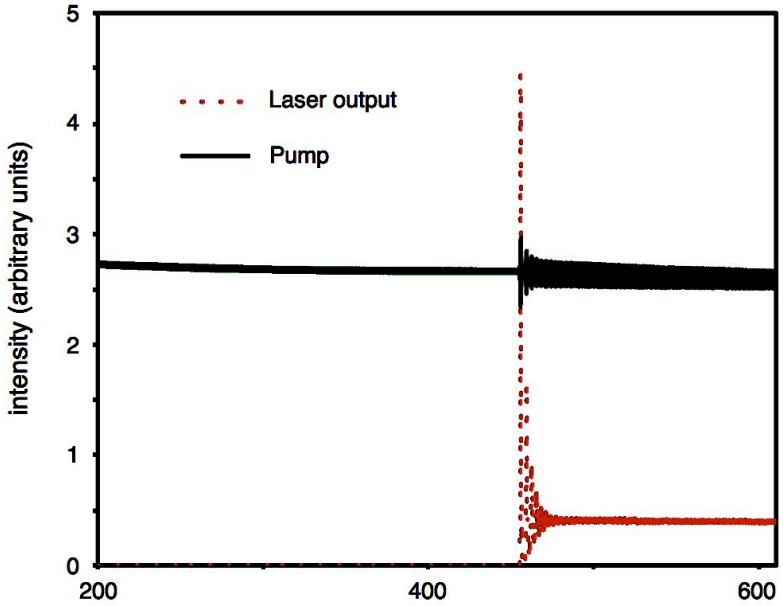

Intensity output of the pump and laser output signals

Source: Chang and Taflove, *Optics Express*, 2004.

Advanced Multi-Level Multi-Electron Model for FDTD Simulation of Semiconductor Materials

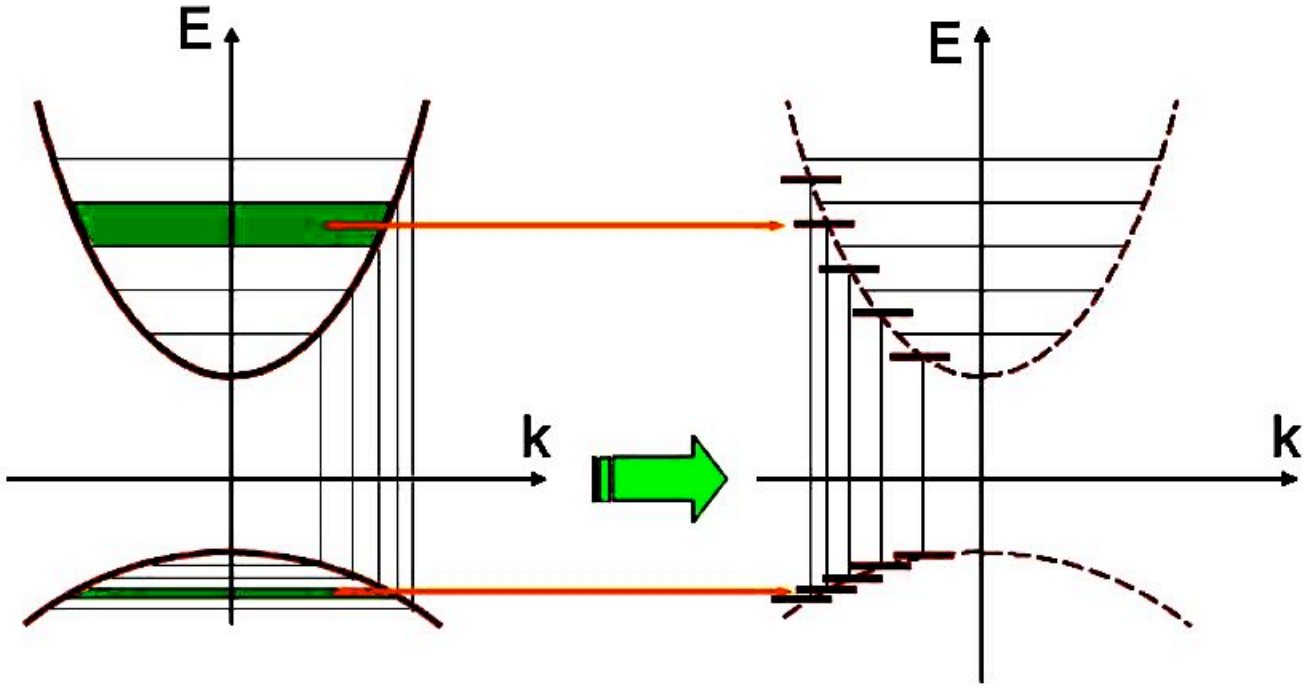

Source: Huang and Ho, *Optics Express*, April 17, 2006, pp. 3569–3587.

2-D Multi-Level Multi-Electron Model of 2-μm Diameter Microdisk Laser

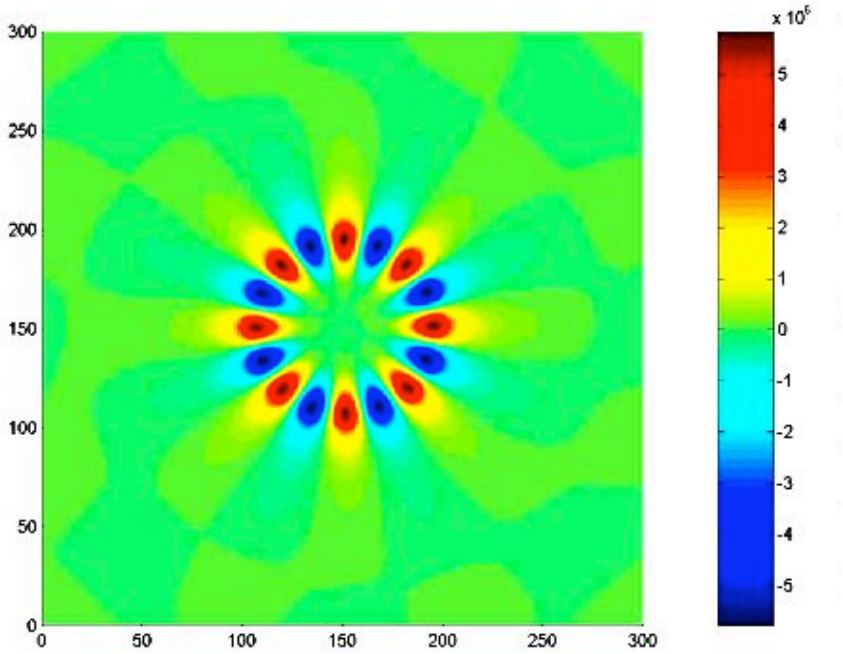

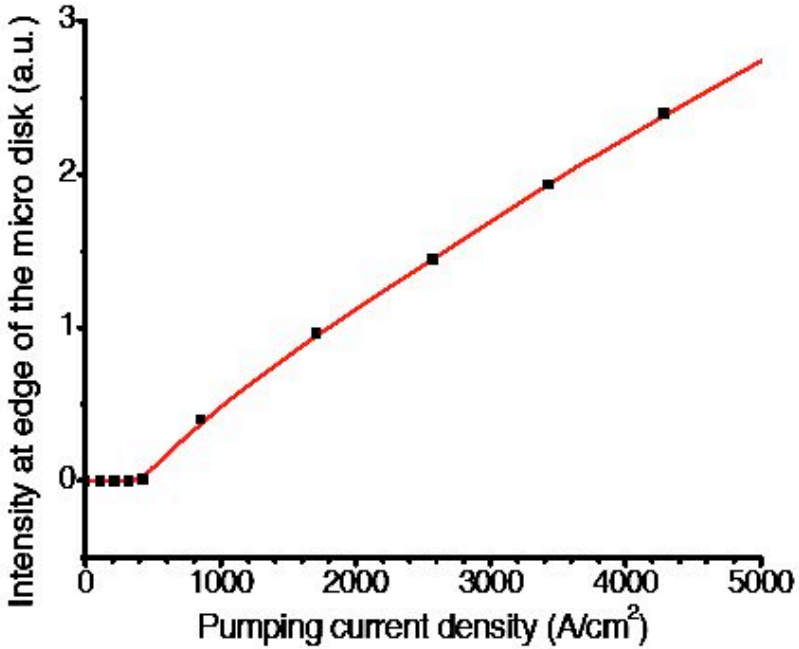

Source: Huang and Ho, *Optics Express*, April 17, 2006, pp. 3569–3587.

Lasing Spectra of the 2-μm Diameter Microdisk Laser at Different Injection Current Densities

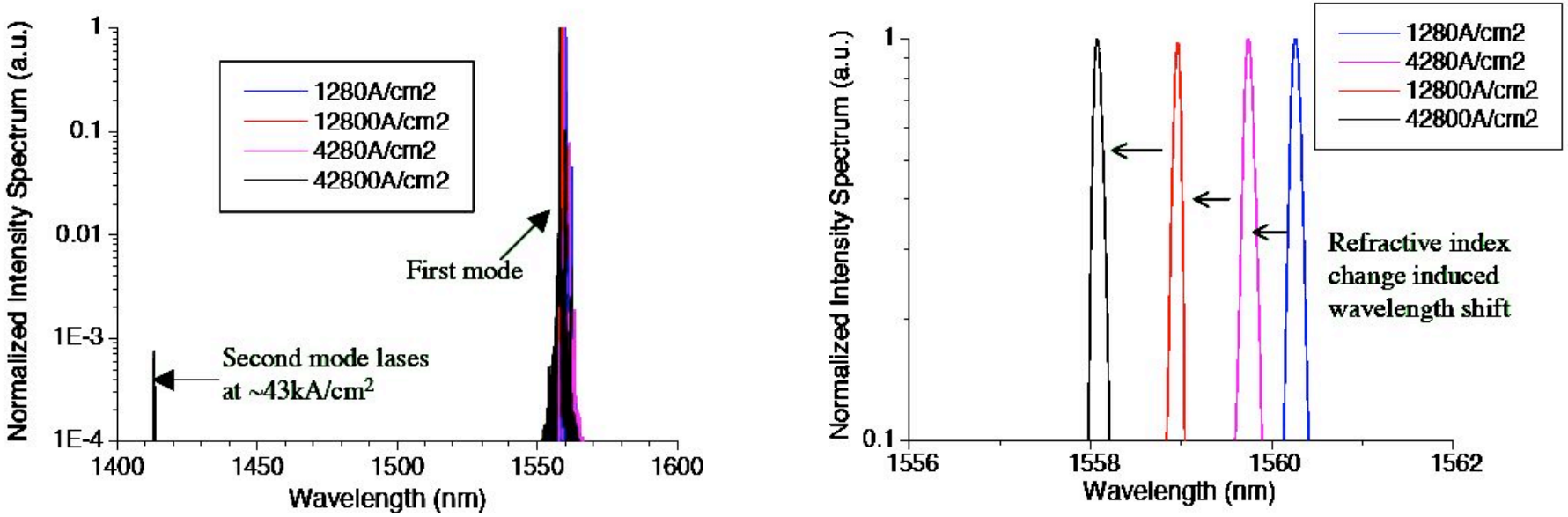

Source: Huang and Ho, *Optics Express*, April 17, 2006, pp. 3569–3587.

Biophotonics

FDTD / PSTD Biophotonics Thrust Areas

- Optical detection of early-stage cancers (colon, pancreas, lung, esophagus)
- Ultramicroscopy of individual living cells to investigate physiological processes

What is the Difference Between These Three Human Colon Cells (observed using conventional microscopy)?

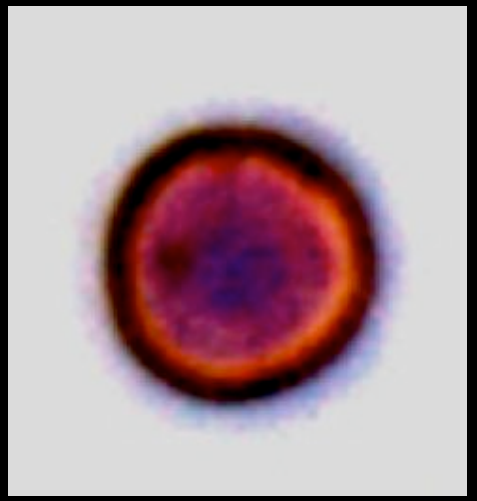

Hint: Two of these cells have the potential to **kill** their human host.

Backscattering Spectroscopy

My Northwestern University colleague and collaborator, Prof. Vadim Backman, has shown that observing the spectrum of retro-reflected light from colon tissues yields much more information regarding pre-cancerous conditions than *any* previous diagnostic technique.

Backscattering Detection of Nanoscale Features

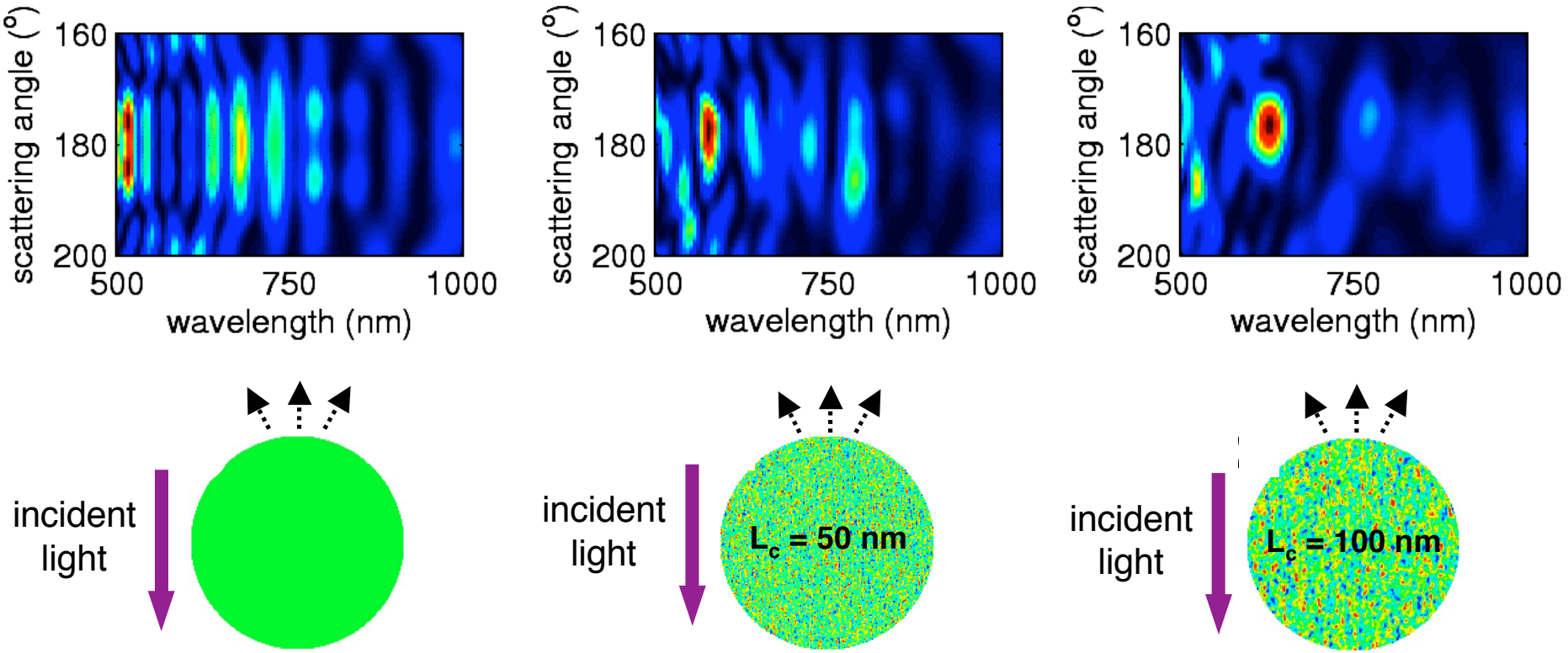

Subdiffraction inhomogeneities generate “fingerprints” in plots of the backscattered spectral intensity versus angle near 180˚.

Source: Li et al., *IEEE JSTQE*, July/Aug. 2005, pp. 759-765.

Emerging Clinical Application

First in lab experiments with rats and then in pre-clinical trials involving hundreds of human subjects, Prof. Backman applied this idea to develop extraordinarily sensitive, accurate, and virtually noninvasive tests for early-stage colon cancer.

Bulk Backscattering Spectral Changes Provide the Earliest Known Colon Cancer Markers in Rats

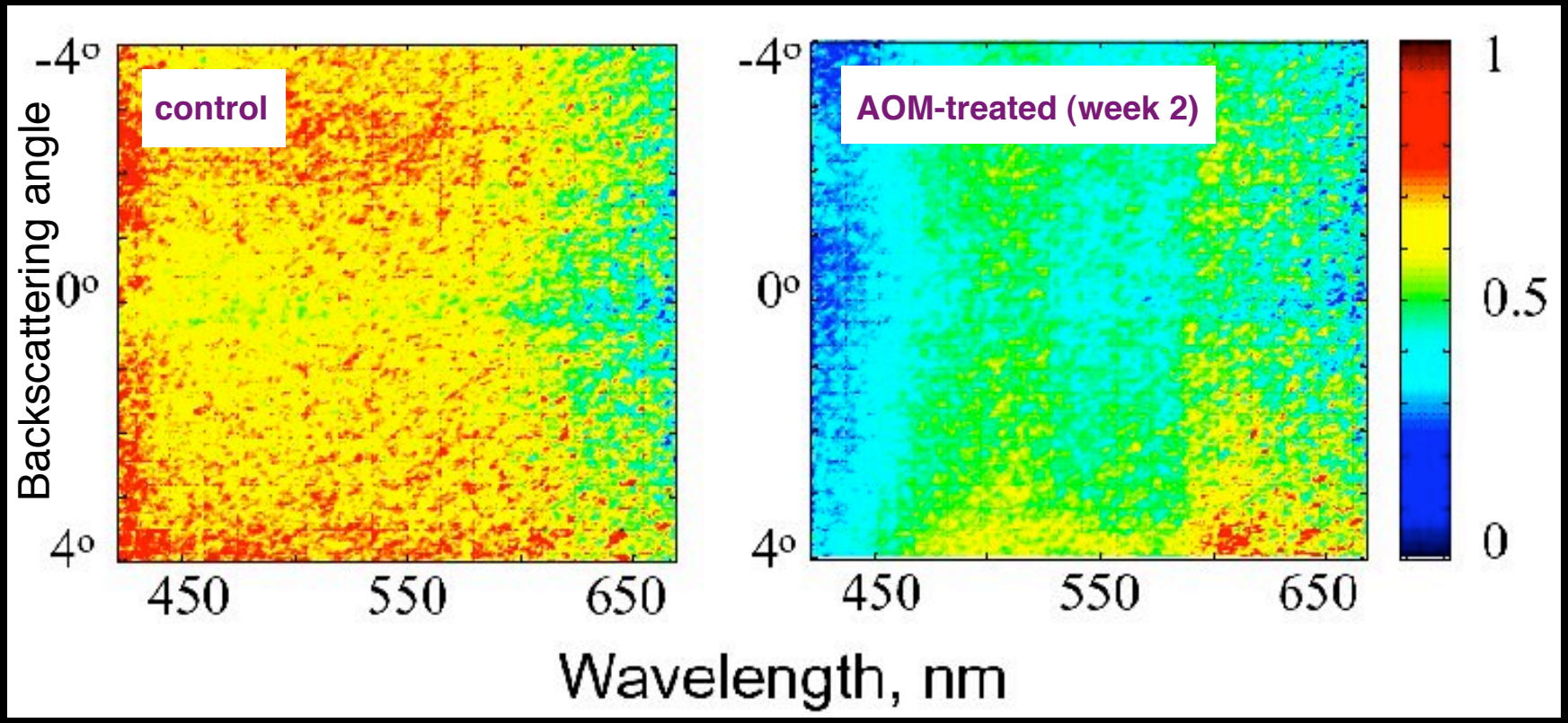

Source: *Gastroenterology*, 126, 1071-1081 (2004).

Current Work: Backscattering Spectroscopic Analysis On a Pixel-by-Pixel Basis ("*Partial-Wave Spectroscopic Microscopy*")

Using FDTD simulations to guide experiments, we are pushing this concept even further to acquire the spectra of individual pixels of a backscattering microscope image.

This will allow monitoring the physiological processes involved in the progression of pre-cancerous conditions at points within a single cell.

Step 1: Show Agreement of Recorded and FDTD-Calculated Backscattering Microscope Images

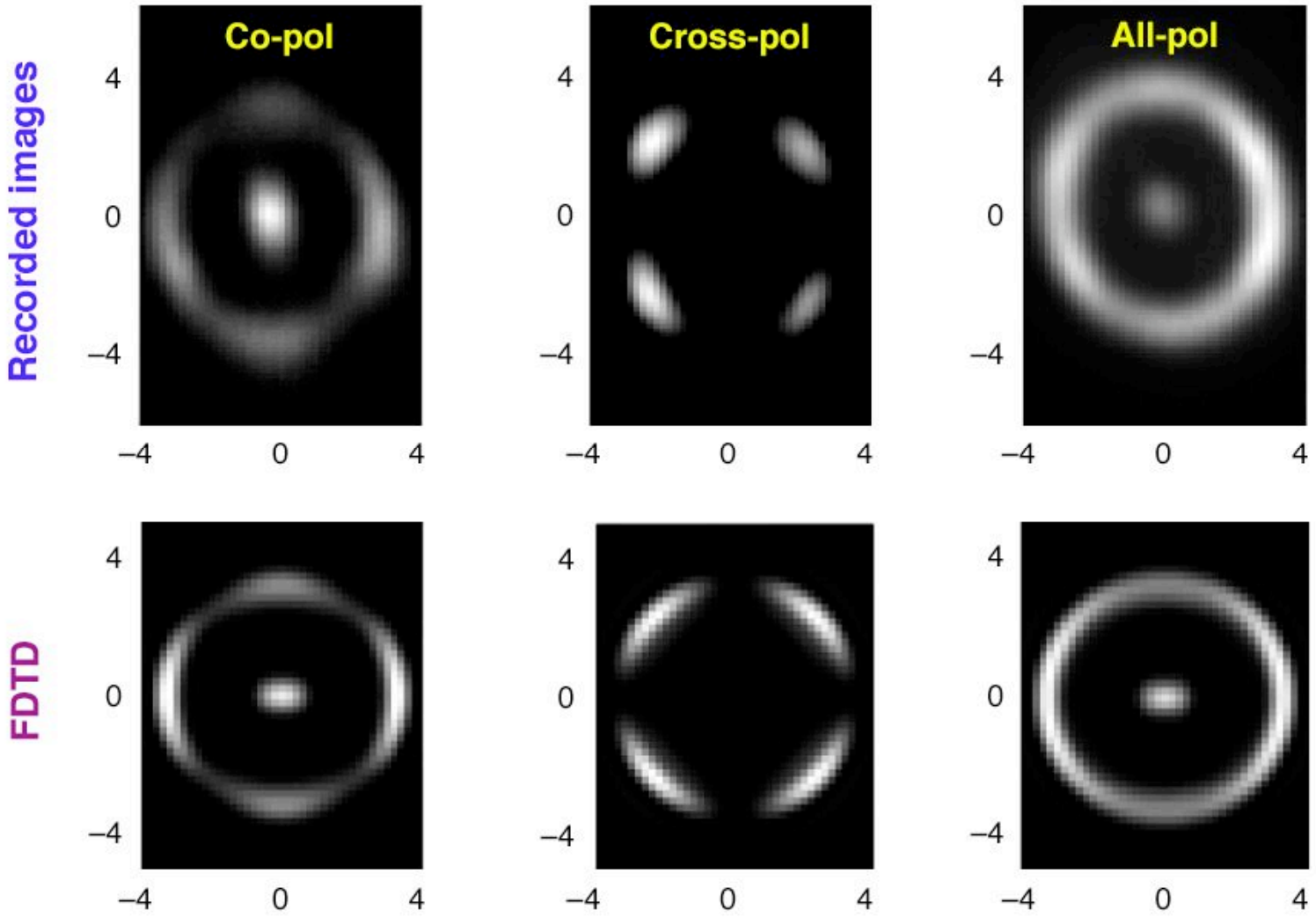

All scales are in μm

Step 2: Apply FDTD to Calculate Spectra of Individual Pixels of Backscattered Microscope Images of Layered Media Having Lateral Inhomogeneities Near the Diffraction Limit

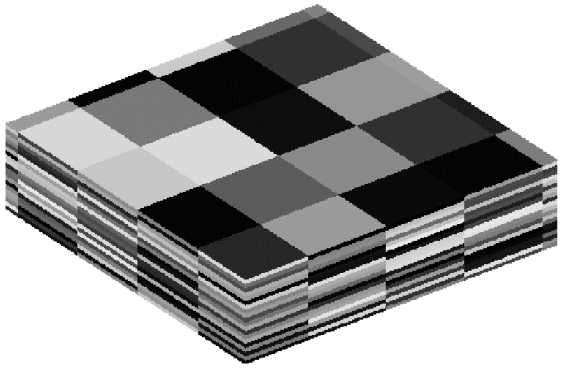

Modeled structure

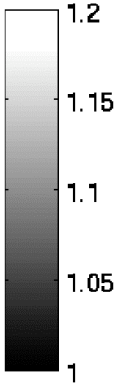

FDTD-calculated image

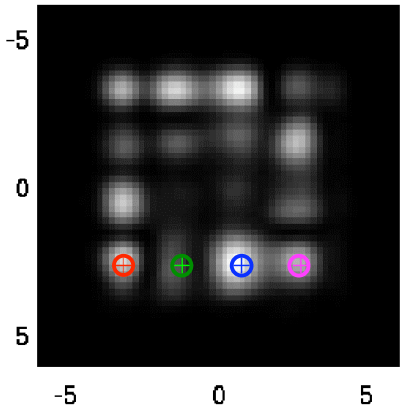

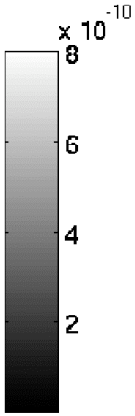

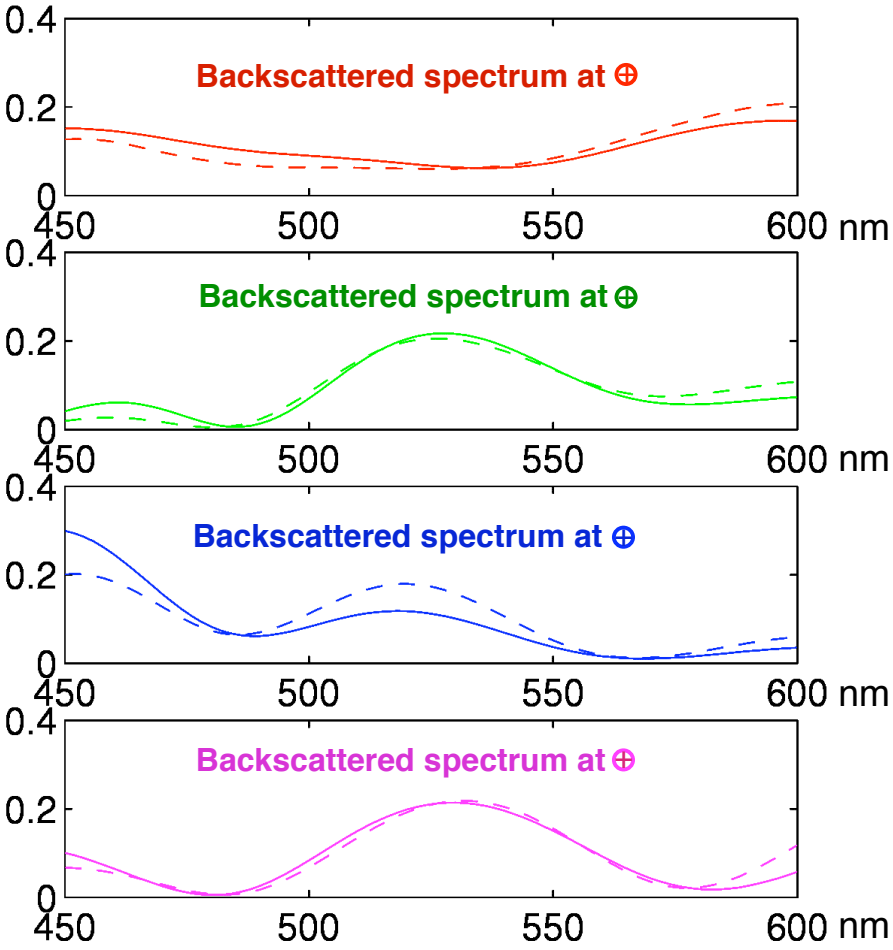

The pixel spectra are strongly correlated with the local 1-D layering in the depth direction.

Using Partial Wave Spectroscopic Microscopy, We Can Now Answer the Question Posed Earlier

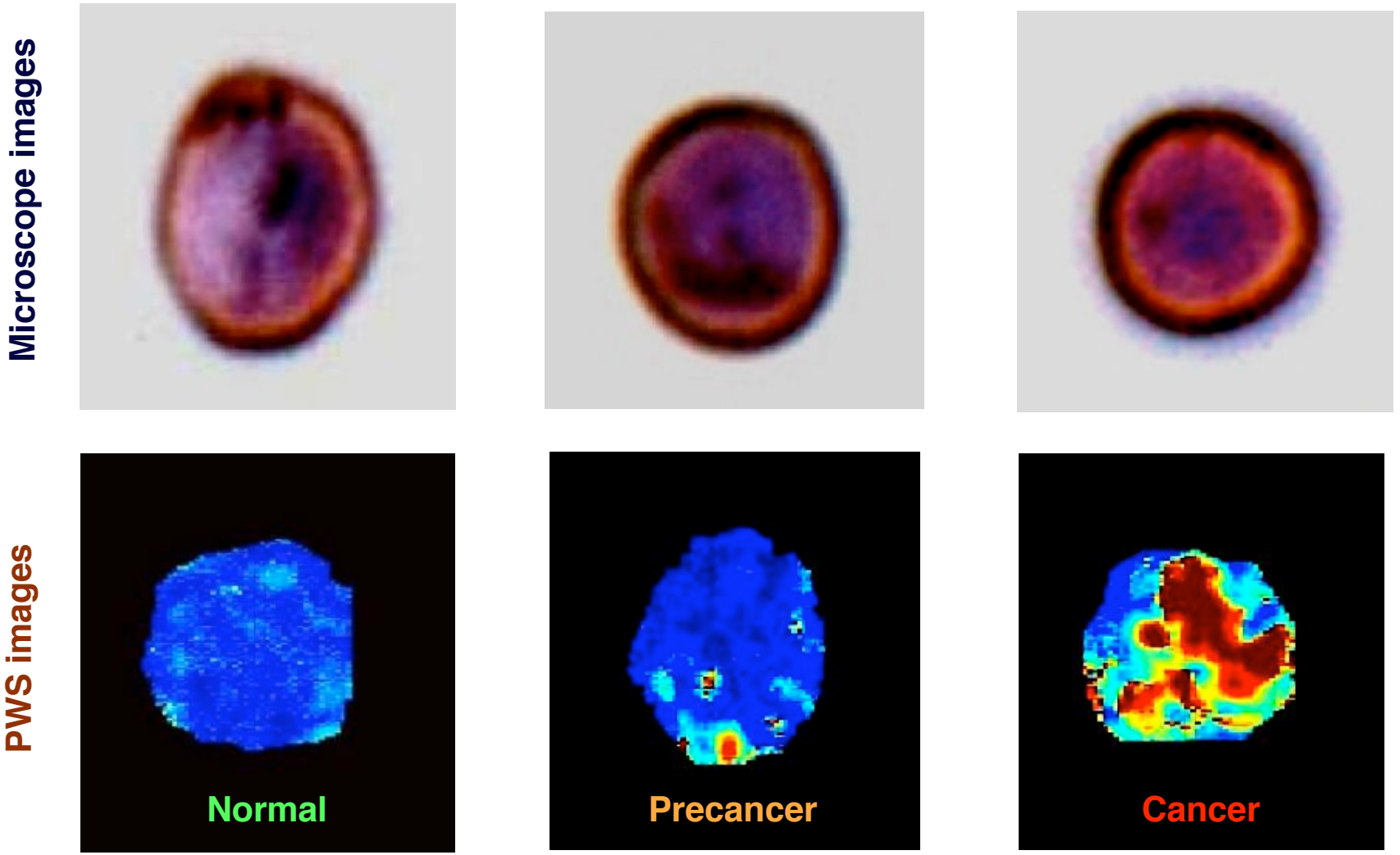

Similar Differentiation is Possible for Human Pancreatic Cancer Cells

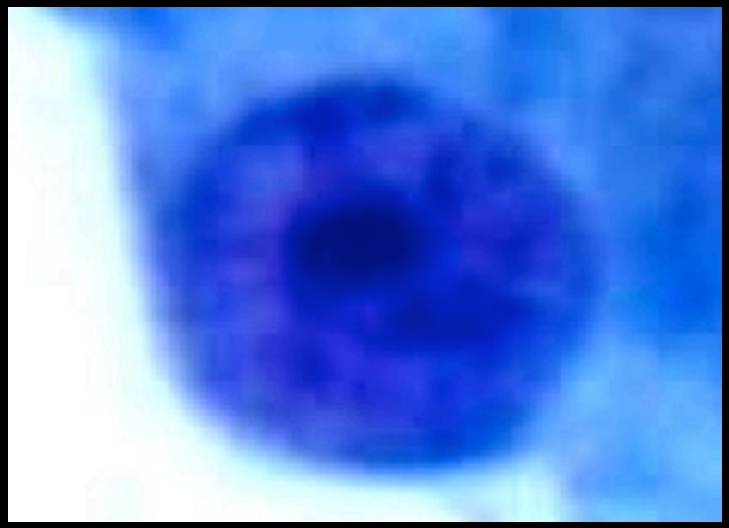

Cytology image

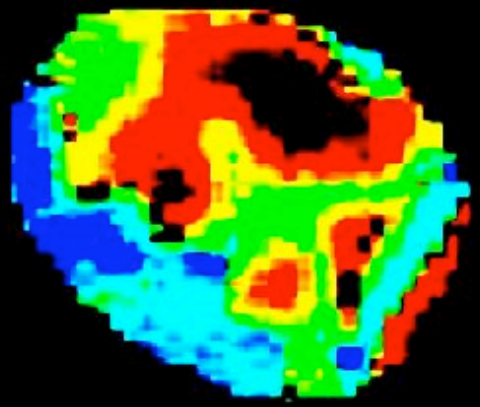

Partial wave spectroscopy image

PSTD Modeling of Clusters of Cells

We are applying PSTD modeling to better understand the interaction of light with large clusters of living cells.

As stated earlier, we are particularly interested in direct backscattering, which appears to convey early indications of cancer.

Validation of Fourier-Basis PSTD for Scattering by a Single Sphere

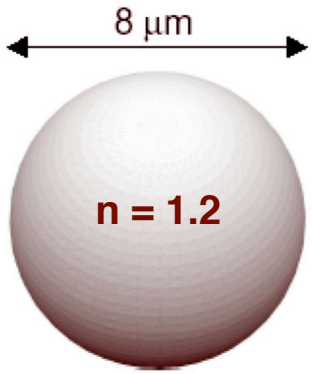

Source: Tseng et al., *Radio Science*, 2006.

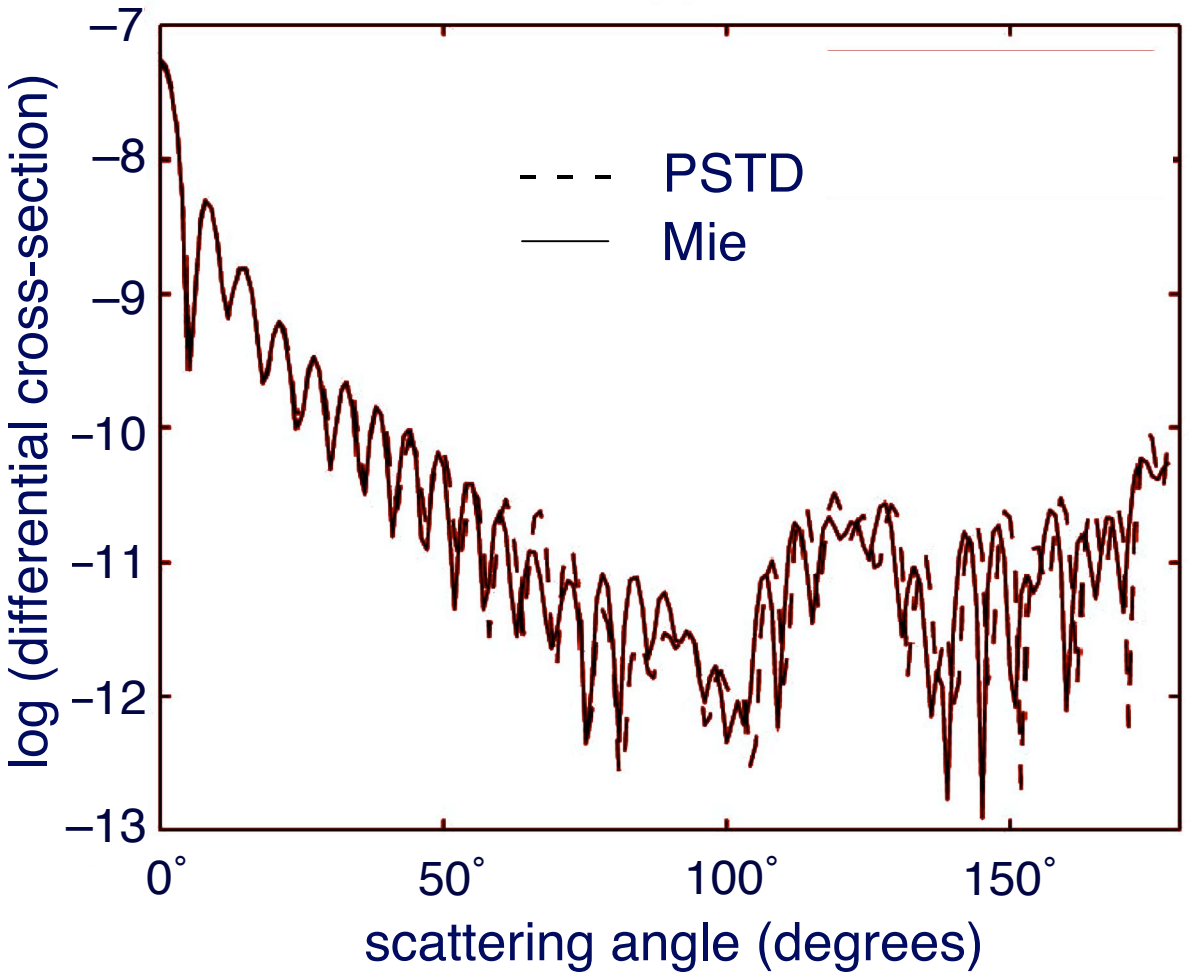

Validation of Fourier-Basis PSTD for Scattering by a 20-μm-Diameter Cluster of 19 Dielectric Spheres

19 spheres, each d = 6 μm and n = 1.2

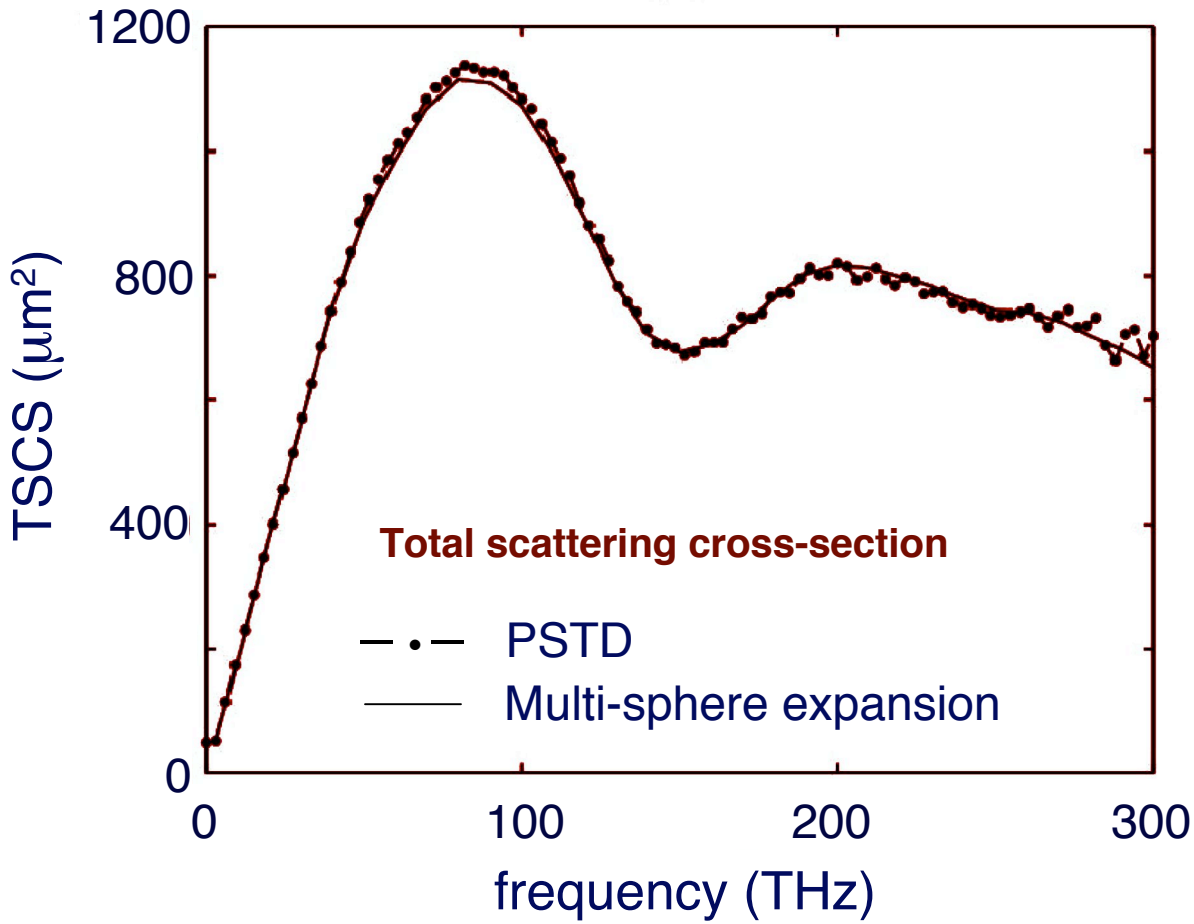

Source: Tseng et al., *Radio Science*, 2006.

PSTD-Calculated Total Scattering Cross-Section of a 25-μm-Diameter Cluster of 192 Dielectric Spheres

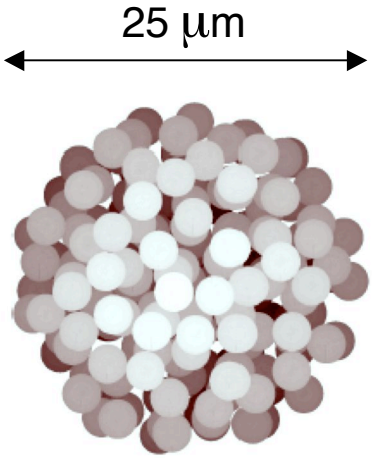

192 spheres, each d = 3 μm and n = 1.2

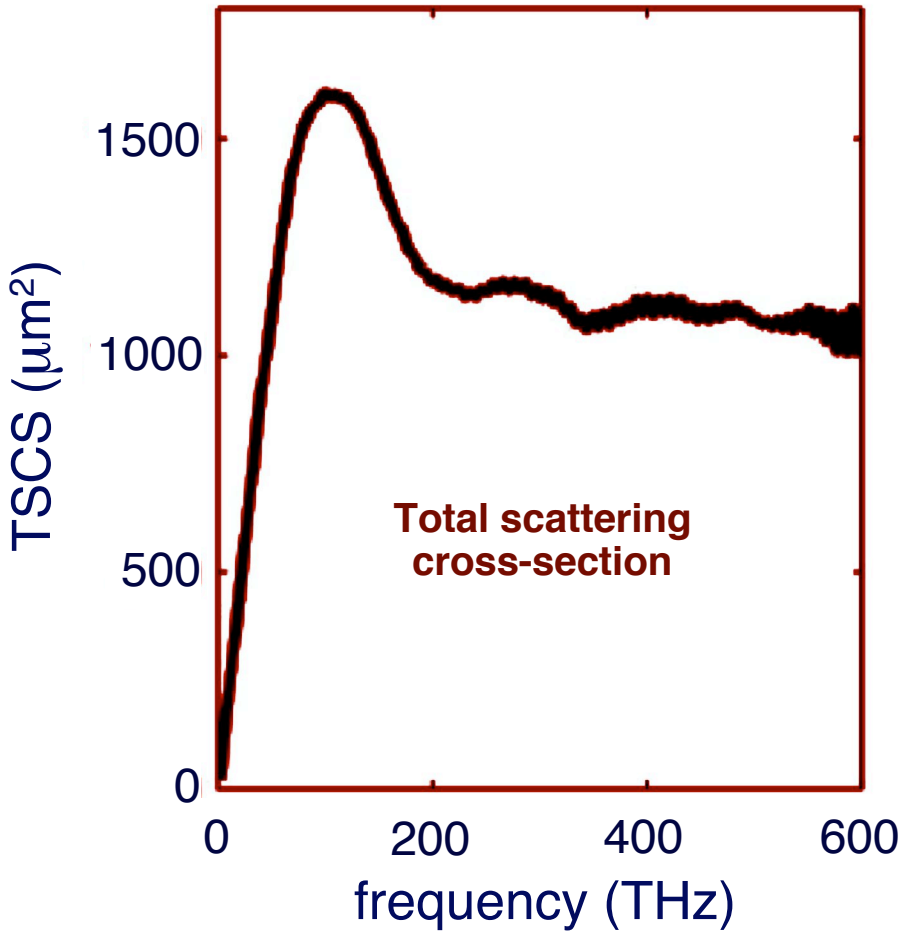

Source: Tseng et al., *Radio Science*, 2006.

Identification of the Component Sphere Size in the 192-Sphere Cluster Via Cross Correlation

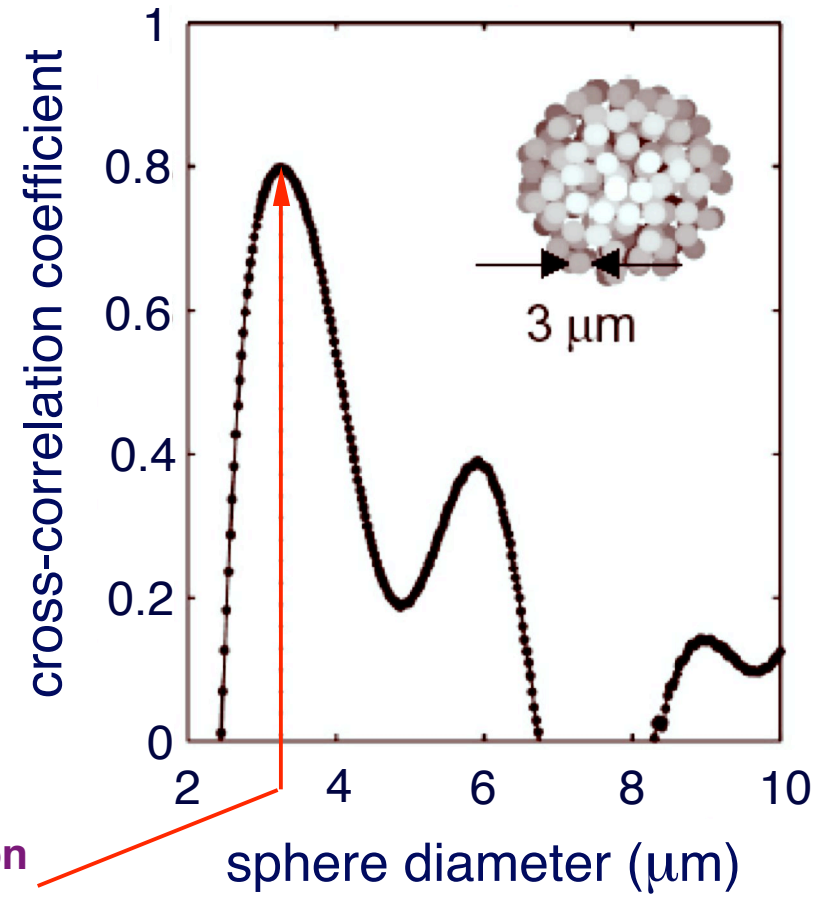

Source: Tseng et al., *Radio Science*, 2006.

Enhanced Backscattering by a Large Cluster of Dielectric Cylinders

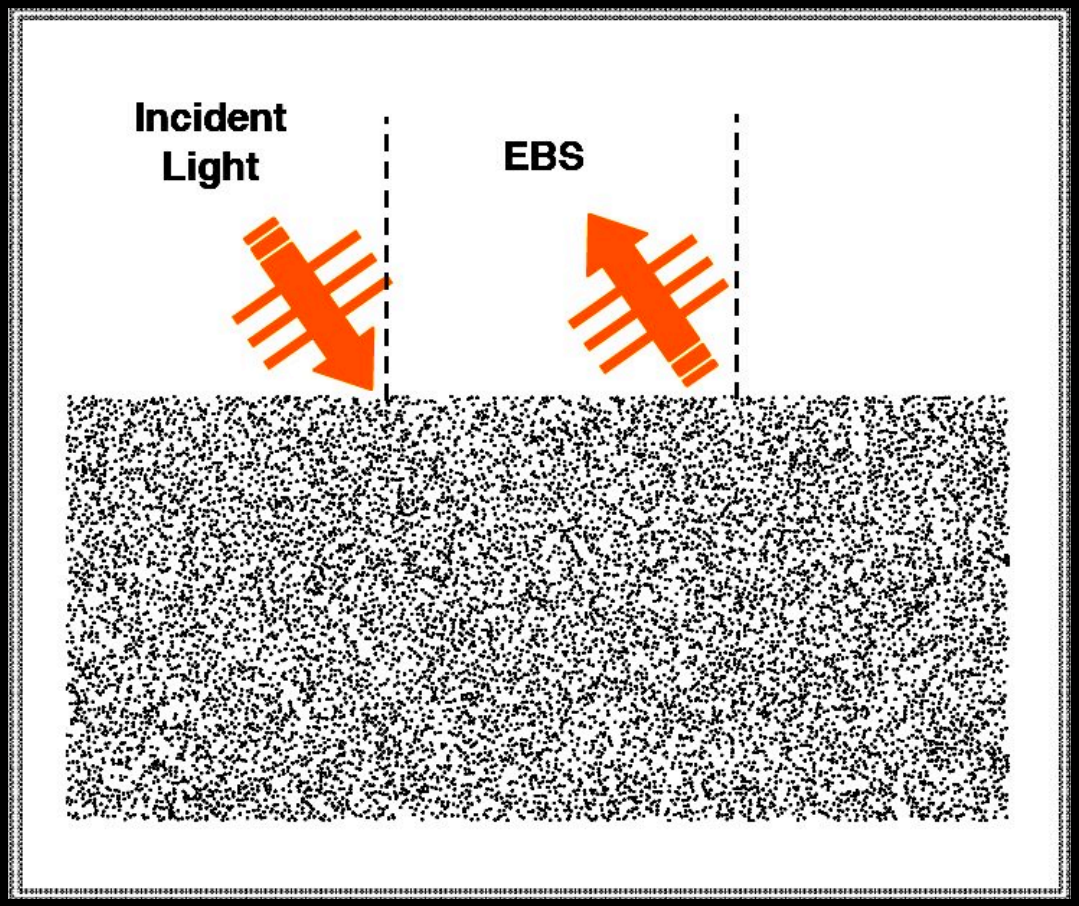

Up to 20,000 randomly positioned, non-contacting, 1.2 μm diameter dielectric cylinders (n = 1.25) packed into an 800 × 400 μm area.

TM-polarized plane-wave illumination at 15° relative to the normal. Far-field back-scattering is calculated.

Source: Tseng et al., *Optics Express*, May 16, 2005, pp. 3666-3672.

Validation Relative to Diffusion Approximation

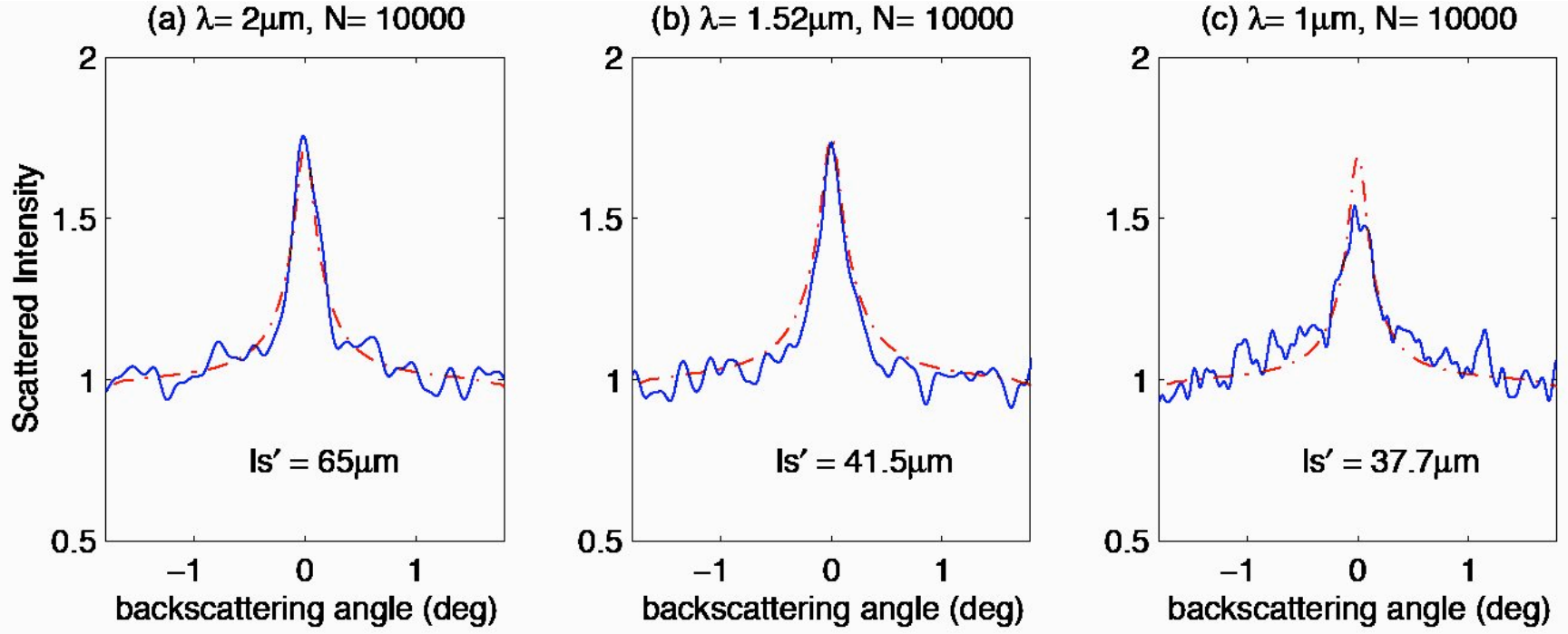

Future Prospects

- Nanophotonics, including as many quantum effects as we can muster. Ultimately, achieve a self-consistent combination of quantum and classical electrodynamics, just as Nature does.
- Biophotonics, especially as applied to the early-stage detection of dread diseases such as cancer.

My Personal Journey

I've been privileged to participate in the advancement of FDTD theory, techniques, and applications over the past 36 years.

It is very gratifying to see the current general widespread usage of FDTD for engineering and science applications that could not have been envisioned back in the 1970's and 1980's.

Thanks for inviting me!